

UC Davis

UC Davis Electronic Theses and Dissertations

Title

Bone Adaptation to Disuse in Aging Rodents: Age-Related Differences in Response to Mechanical Unloading and Subsequent Reloading

Permalink

<https://escholarship.org/uc/item/62c5m4s0>

Author

Cunningham, Hailey Cameron

Publication Date

2021

Peer reviewed|Thesis/dissertation

Bone Adaptation to Disuse in Aging Rodents: Age-Related Differences in Response to
Mechanical Unloading and Subsequent Reloading

By

HAILEY CAMERON CUNNINGHAM
DISSERTATION

Submitted in partial satisfaction of the requirements for the degree of

DOCTOR OF PHILOSOPHY

in

Biomedical Engineering

in the

OFFICE OF GRADUATE STUDIES

of the

UNIVERSITY OF CALIFORNIA

DAVIS

Approved:

Blaine Christiansen, Chair

Susan Stover

Damian Genetos

Keith Baar

Committee in Charge

2021

Acknowledgements

The PhD journey has been one of the most rewarding and difficult things I have ever done, and it is a journey that is impossible to do alone. There are so many people who I would like to thank as it ends.

First, I want to thank Dr. Maritoni Litorja at the National Institute of Standards and Technology for my first research experience and for encouraging me to take on the PhD program in the first place. I would also like to thank my professors at my undergraduate institution, George Washington University for their support and guidance.

Next, I must thank my committee, other faculty members and collaborators at the University of California, Davis. Dr. Susan Stover, Dr. Damian Genetos and Dr. Keith Baar as committee members and collaborators, have helped guide my research through these years and provided valuable assistance on many topics. I have worked with so many other collaborators and professors who I have met during this program who have helped shape me as a researcher and scientist.

The members of the Christiansen Lab, past and present have also been some of my biggest supporters through the years. Dr. Blaine Christiansen has provided so much support as I worked my way through becoming a researcher and developing a project. Current and past members of the lab including Dr. Allison Hsia, Dr. Armaun Emami, Dr.

Benjamin Osipov, Priscilla Tjandra and so many others have helped with everything from extra hands during procedures to working through difficult research questions and I am so grateful to have been in such a supportive lab.

The friends I made while in Davis have been some of the closest friends I have ever had. From the friends who were also pushing through a PhD themselves to the friends who were supportive from the sidelines, having such a wide support system meant that I always had help when I needed it.

My family may not have always known what exactly I was doing but has never been anything but supportive in everything that I have attempted. I am grateful that my parents instilled in me a drive to push for the top of whatever I set my mind to, and they have always been a source of inspiration to me. Even the furry members of my family, my two cats, have done their part, encouraging me to take breaks since they are far more important than I am anyways.

My largest thank you goes to my husband, Peter, who has been with me through the highest and lowest points of this whole endeavor. He has sat through far too many discussions of biology and bones for an automotive engineer, with only minimal complaints. He has been my greatest ally through everything, from research triumphs to late night panics. There are no words that describe how important his support has been throughout this program.

Table of Contents

Acknowledgments	ii
Table of Contents	iv
List of Figures	v
List of Tables	viii
Abstract	ix
Chapter 1: Background	
1.1 Significance: Skeletal fragility in elderly patients	1
1.2 Bone turnover	2
1.3 Bone mechanotransduction	4
1.4 Regulation of bone turnover	7
1.5 Disuse in bone	8
1.6 Role of osteocytes in disuse induced bone loss	10
1.7 Bone recovery following disuse	12
1.8 Aging and bone	14
1.9 Disuse in aged bone	17
1.10 Summary and knowledge gap	18
Chapter 2: Age-dependent recovery of bone during reloading following a period of hindlimb unloading in rats	
2.1 Abstract	20
2.2 Background	21
2.3 Methods	
2.3.1 Animals	24

2.3.2 Experimental groups and study design	24
2.3.3 Hindlimb unloading via tail suspension	26
2.3.4 Cage activity	26
2.3.5 Micro-computed tomography analysis of trabecular and cortical bone	27
2.3.6 Three-point bending mechanical testing	27
2.3.7 Metaphysis trabecular bone compression	28
2.3.8 Statistical analysis	29
2.4 Results	
2.4.1 Animals	30
2.4.2 Micro-computed tomography analysis of trabecular bone	30
2.4.3 Micro-computed tomography analysis of cortical bone	33
2.4.4 Three-point bending mechanical testing	34
2.4.5 Trabecular bone compression	35
2.5 Discussion	37
2.6 Conclusions	43
2.7 Acknowledgements	44
Chapter 3: Differential bone adaptation to mechanical unloading and reloading in young, old and BCL-2 transgenic mice	
3.1 Abstract	45
3.2 Introduction	46
3.3 Methods	
3.3.1 Animals	50
3.3.2 Experimental groups and study design	51

3.3.3 Hindlimb unloading via tail suspension	52
3.3.4 Histology	53
3.3.5 Micro-computed tomography analysis of trabecular and cortical bone	53
3.3.6 Mechanical testing	55
3.3.7 Serum cytokine analysis	55
3.3.8 Statistical analysis	56
3.4 Results	
3.4.1 Histology: TUNEL Staining	57
3.4.2 Micro-computed tomography analysis: Young WT mice	59
3.4.3 Micro-computed tomography analysis: Old WT mice	62
3.4.4 Micro-computed tomography analysis: Young BCL-2 Tg mice	66
3.4.5 Mechanical testing	69
3.4.6 Serum cytokine analysis	73
3.5 Discussion	75
3.6 Conclusions	87
Chapter 4: Conclusions and future directions	88
References	93

List of Tables

Table 3.1: Experimental groups, terminal time points for subgroups, and subgroup sizes	52
Table 3.2: Young WT μ CT analysis data	60
Table 3.3: Old WT μ CT analysis data	63
Table 3.4: Young BCL-2 Tg μ CT analysis data	66
Table 3.5: Mechanical testing data	70
Table 3.6: Serum cytokine ELISA data	74

List of Figures

Figure 1.1: Regulation of bone turnover	3
Figure 1.2: Bone adaptation via modeling and remodeling with respect to strain	6
Figure 1.3: Tail suspension in rats	9
Figure 2.1: Experimental design	25
Figure 2.2: Distal femoral metaphysis trabecular bone tissue μ CT results	31
Figure 2.3: Metaphyseal trabecular bone structure of additional aged groups	32
Figure 2.4: Mid-femoral diaphysis cortical μ CT results	34
Figure 2.5: Three-point bending results	35
Figure 2.6: Trabecular bone compression results	36
Figure 3.1: TUNEL staining in representative baseline samples	58
Figure 3.2: Normalized number of live and dead osteocytes and empty lacunae	59
Figure 3.3: Comparison of Young WT and Old WT μ CT results	65
Figure 3.4: Comparison of Young WT and Young BCL-2 Tg μ CT results	68
Figure 3.5: Comparison of Young WT and Old WT 3-point bending results	72
Figure 3.6: Comparison of Young WT and Young BCL-2 Tg 3-point bending results	73
Figure 3.7: Serum cytokine ELISA results	75

Abstract

Adaptation of the bones of older subjects to disuse is largely unknown and bone recovery following disuse in older subjects has not been studied. Up to half of all people over the age of 50 suffer from osteoporosis or low bone mass and older patients are more vulnerable to extended hospitalizations. With advancing age, bone experiences an age-related decline through trabecular bone loss, cortical thinning, and decreased osteocyte density. Decreased osteocyte density could contribute to the impaired adaptation of older bones to increased loading. This could affect an older subject's ability to recover from disuse-induced bone loss. In this research we sought to quantify bone adaptation of young and old rats and mice in response to mechanical unloading via tail suspension and subsequent reloading. In addition, we aimed to compare the bone adaptation of old mice to a transgenic mouse model of low osteocyte density to determine the effect of osteocyte density on bone adaptation in response to mechanical unloading and reloading. We found that young rats lost trabecular bone quickly during unloading but recovered after only a short period of reloading. Meanwhile, old rats did not lose bone during unloading but did lose trabecular bone during early reloading that did not recover with continued reloading. In mice, we found that young, old, and transgenic mice all lost trabecular bone during unloading but young mice recovered more bone during reloading than old or transgenic mice. Old mice also lost cortical bone during unloading and reloading while transgenic mice lost no cortical bone. These results illustrate a difference in bone adaptation between different ages of mice and rats and further research into this difference may provide valuable insights for protecting the skeletal health of the elderly.

Chapter 1: Background

1.1 Significance: Skeletal fragility in elderly patients

Skeletal fragility in elderly patients is a consistent health concern due to age-related decreases in bone structure and strength. Osteoporosis is a metabolic bone condition involving an imbalance between rates of bone resorption and bone formation leading to reduced bone mineral density (BMD) with a greatly increased fracture risk in elderly people¹. It is estimated that approximately half of all adults over the age of 50 have a significant risk of fracture due to osteoporosis and low bone density². Many health conditions that disproportionately affect elderly patients have negative effects on the strength of the skeletal system and can lead to secondary osteoporosis, either as a result of an underlying condition (such as in chronic kidney and liver disease) or as a result of treatment for the condition as seen in radiation treatment for various forms of cancer³. Bone loss also occurs during periods of low mechanical loading (disuse) as bone is highly responsive to changes in the mechanical environment. Older people make up a disproportionately high percentage of hospitalizations, and their hospitalizations are significantly longer on average than that of a younger person^{4,5}. Periods of disuse associated with hospitalization in the elderly can therefore threaten an already weakening skeletal system. However, there is a lack of information on the ability of bone of older subjects to adapt to disuse and subsequent recovery. Due to increasing skeletal fragility with age, it is important to understand whether mechanisms that compromise bone health such as extended periods of disuse differentially affect older subjects.

1.2 Bone turnover

Bone turnover occurs by two major processes; bone modeling, in which bone is resorbed or formed independently and changes the overall size and/or shape of the bone, and bone remodeling in which bone resorption and formation occur sequentially to remove older bone tissue and form new bone tissue in the same location without changing the overall size and/or shape of the bone⁶. Normal physiological loading of bone over time will result in microdamage to the bone tissue in the form of microcracks that occur with repetitive loading⁷. Bone remodeling is critical for bone to heal from accrued microdamage and for bone to adapt to a change in loading environment.

Bone remodeling involves the coordinated actions of osteoclasts, osteoblasts, and osteocytes. The bone remodeling cycle begins with the activation of osteoclasts. Osteoclasts are multinucleated cells that attach and seal themselves to bone surfaces and resorb bone by releasing enzymes and acid in the sealed area⁶. Osteoclasts and their precursors are derived from the hematopoietic stem cells (HSC) in bone marrow^{8,9}. In bone remodeling, circulating mononuclear preosteoclasts migrate to the targeted bone surface through blood vessels and coalesce into multinucleated osteoclasts where they begin to resorb bone. After bone resorption, pre-osteoblasts migrate to the resorption bays and differentiate into mature osteoblasts during the reversal phase from bone resorption to bone formation⁶. Osteoblasts and their precursors are derived from the mesenchymal stem cells of bone marrow⁸. Osteoblasts begin to form bone by laying down unmineralized bone matrix called osteoid, which will mineralize over time to form mature bone tissue. During the process of laying down new bone, some osteoblasts will

become trapped in the osteoid and will become osteocytes, embedded in the newly mineralizing tissue^{6,9}. Osteocytes are considered the major force sensing cells in bone. Force is sensed through fluid flow within their extensive canalicular networks. Osteocytes produce signaling molecules that regulate osteoclast and osteoblast activity¹⁰⁻¹². Once bone formation has completed and the new bone has mineralized, the current cycle bone remodeling is complete and the tissue enters a state of quiescence until a new bone remodeling cycle is induced⁶.

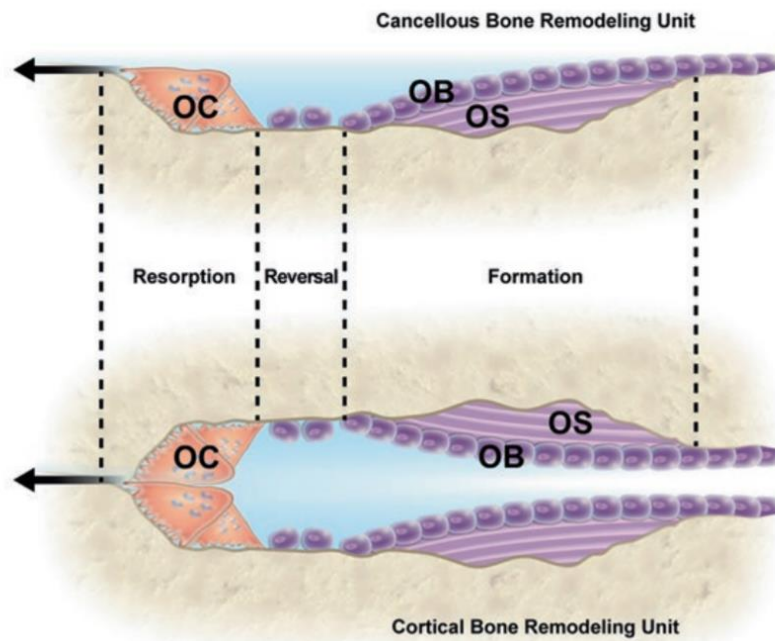


Figure 1.1: Bone turnover. Illustration of BMU in trabecular and cortical bone remodeling. Bone remodeling involves coordinated actions of osteoclasts (OC) resorbing bone and osteoblasts (OB) laying down new osteoid (OS). Illustration adapted from Gasser and Kneissel 2017¹³.

During remodeling, osteoclast and osteoblast activity occur simultaneously in super-structures called bone multicellular units (BMUs)^{6,8} (Fig. 1.1). In dense compact bone such as cortical bone, these BMUs forms in a cylindrical structure called an osteon

that tunnels through cortical bone with several osteoclasts resorbing bone at the front and osteoblasts laying down osteoid at the rear. In trabecular bone, individual trabeculae are often thinner than a BMU and thus the BMU will resorb and reform a scalloped shape on the surface of trabecula^{6,8}. The duration a bone remodeling cycle differs based on the subject. In adult humans, one full bone remodeling cycle lasts around 200 days, with bone resorption lasting 30-40 days, bone formation lasting around 150 days^{6,14,15}. The duration of bone remodeling can be affected by different bone conditions or treatments. Conditions such as hyperparathyroidism can greatly decrease the cycle duration while the duration the bone remodeling cycle can be greatly increased by the use of bisphosphonates¹⁴. In rodents, the duration of the bone remodeling cycle is significantly shorter, lasting on average 14 days in an adult mouse^{16,17} and around 36 days in an adult rat^{18,19}.

1.3 Bone mechanotransduction

Bone tissue is very biologically active and is constantly replacing itself. Bone structure is highly optimized to maximize strength of bone under expected loads while minimizing the weight of the overall bone structure⁶. Scientists have described this phenomenon in a variety of ways, including Wolff's Law and Frost's bone mechanostat model.

Wolff's law describes how a theoretical ideal bone structure would adapt in response the mechanical loads it experiences²⁰. The main principles of Wolff's law are that bone will optimize strength with respect to weight, that trabeculae within cancellous

bone will organize themselves with principal stress directions and that bone structure self-regulates by cells responding to mechanical loads^{6,21}.

Frost's mechanostat theory of bone attempts to explain the nature of how bone adapts to mechanical stimuli⁶ (Fig. 1.2). As bone experiences a mechanical load, it deforms slightly as a result, causing a mechanical strain. Frost's theory postulates that there is an equilibrium range of maximum strain magnitude experienced by bone in which no net gain or loss of bone will occur. For net bone gain or loss to occur, strains on the bone must fall outside this equilibrium range. Higher strains will result in a positive bone adaptation, accumulating bone. Lower strains will result in a negative bone adaptation, losing bone^{22,23}. In lower strain environments, Frost proposes that remodeling will increase and modeling will decrease while in higher strain environments he proposes that modeling will increase and remodeling will decrease²⁴. These theories together describe bone's response to high and low strain environments by accumulating or losing bone, respectively, to adapt to its current loading environment and to optimize the internal microstructure to maximize bone's strength to weight ratio.

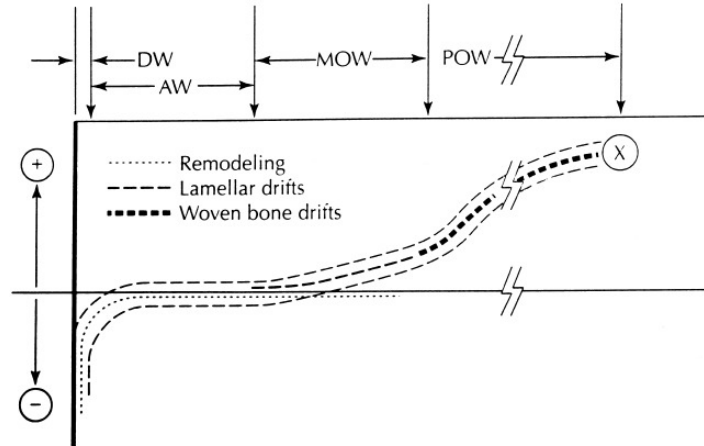


Figure 1.2: Bone adaptation via modeling and remodeling with respect to strain magnitude. Across the top, strain on the bone indicates the adaptation window of the bone. From left to right the regions are: the very low strain disuse window (DW) in which bone is lost, the normal adapted window (AW) in which little adaptation occurs, the mildly overworked window (MOW) where bone will accumulate and the pathological overwork window (POW) in which injury or fracture (X) is a high probability. The vertical axis indicated a positive (above the axis) or negative (below the axis) adaptive response in bone. Figure taken from Frost, 1960²⁴.

Wolff's law and Frost's mechanostat theory describe the manner by which bone adapts to mechanical loads. One mechanism by which bone senses these loads is the osteocytes distributed throughout the bone matrix and the lacunar-canalicular network that runs throughout the bone and connects them^{25,26}. Osteocytes lie within lacunae within the bone matrix and are connected to other osteocytes by osteocyte processes within the branching fluid-filled canalicular network. There is evidence that when the bone experiences a mechanical load, a fluid flow in the canalicular network of the bone is induced which osteocytes are able to sense²⁷⁻²⁹. Thus, osteocytes can sense the mechanical load and, through the release of different signaling molecules, can affect the rate of bone resorption and bone formation by regulating of the activity of osteoclasts and osteoblasts^{10,12}.

1.4 Regulation of bone turnover

The different cells involved in bone formation and resorption are regulated through a variety of signals including activity of other bone cells. Osteoclast activity is stimulated by inflammatory cytokines and other signaling molecules. Receptor activator of NF-kappa B ligand (RANKL) is the primary regulator of osteoclast activity⁸. RANKL is produced largely by osteocytes and osteoblasts and helps to stimulate the differentiation of new osteoclasts from hematopoietic stem cells (HSCs) in the bone marrow while suppressing apoptosis of osteoclasts⁹. Osteocytes are often the origin of osteoclast activation and are a major bone resorption regulator through their release of RANKL or through osteocyte apoptosis which can also signal osteoclast activation³⁰. Other signaling molecules such as macrophage colony stimulating factor (M-CSF) and vascular endothelial growth factor (VEGF) and inflammatory cytokines such as interleukin 6 (IL-6) and tumor necrosis factor alpha (TNF- α) can also stimulate osteoclast activity^{8,9}. Inhibitors of osteoclast activity include estrogens which reduce osteoclastogenesis and osteoprotegerin (OPG) which acts as a decoy receptor blocking the activity of RANKL^{8,9}.

Osteoblast activity is stimulated by a number of growth factors including bone morphogenetic proteins (BMPs), insulin-like growth factors (IGFs), transforming growth factor beta (TGF- β), and fibroblast growth factor (FGF) among others. The release of these growth factors from the bone matrix may be enhanced by osteolysis during osteoclast activity. In addition, Wnt signaling promotes osteoblast formation and activity. Wnt signaling is inhibited by sclerostin (SOST) which is produced by osteocytes^{8,12}. Parathyroid hormone (PTH) is a regulator of calcium homeostasis and stimulates

osteoblast activity and differentiation⁹. However, although it does not directly act upon osteoclasts, PTH also can increase osteoclast activity by increasing RANKL production from osteoblasts³¹.

1.5 Disuse in bone

Bedrest and spaceflight studies are the two most common methods to examine the effect of mechanical unloading on humans. Studies of skeletal changes in astronauts due to spaceflight are limited in number and involve small sample sizes. Subjects in these studies are more frequently male, and due to spaceflight requirements, subjects are generally relatively young, physically fit, and overall healthy³²⁻³⁵. Dual energy X-ray absorptiometry measurements on astronauts following extended durations in space reveal losses in BMD of 0.9 – 1.06% per month in the spine and 1.0 – 1.6% per month in the hip and femoral neck^{32,33}. Losses in BMD following spaceflight are mirrored in decreased mechanical properties simulated through finite element analysis³⁶. In bed rest studies, trabecular bone is similarly lost after a length of time unloading. Women in a 60 day bed rest study lost 3-4% of trabecular BMD in the femur and tibia³⁷ and men in a 17 week bed rest study lost 1.4% of total body BMD and 2-4% of BMD in specific sites such as the femoral neck and tibia³⁸.

In animal studies, disuse is studied in a variety of methods including tail suspension and spaceflight studies. Spaceflight studies in rodents have found that the bones of mice and rats undergo severe disuse-induced bone loss, mostly in trabecular

bone though cortical bone is affected as well, at a much faster rate than has been seen in humans³⁹⁻⁴³. Mice after a 30 day spaceflight experience 30-60% trabecular bone loss in their tibias and femurs^{44,45}. Meanwhile, rats who underwent a 14 day spaceflight experienced a 30% decrease in trabecular bone volume fraction in the spine⁴⁶.

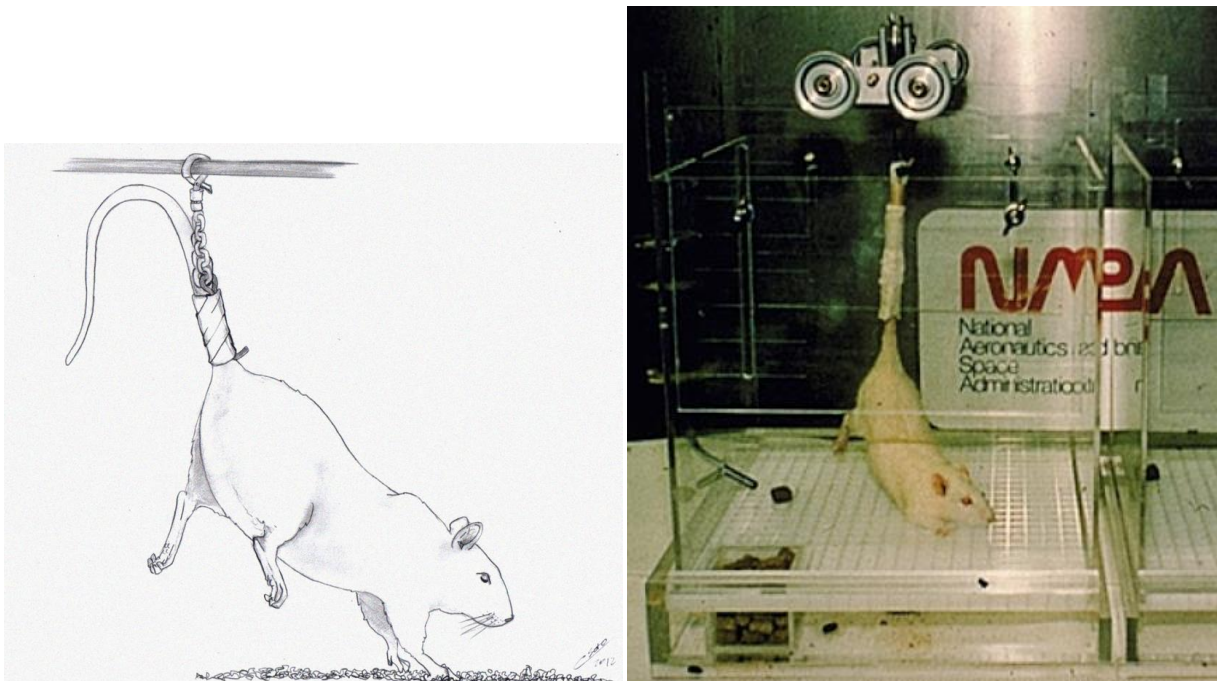


Figure 1.3: Tail suspension in rats. Tail suspension illustration (left) adapted from Marzuca-Nassr et al. 2017⁴⁷. Early image of tail suspension in rats by Wronski et al. 1987⁴⁸.

Unloading via tail suspension was first developed by NASA as an alternate method for examining the effects of simulated microgravity without the need for spaceflight and is one of the major methods to examine mechanical unloading on bone (Fig. 1.3). In this model first established by Morey-Holten, animals are suspended by their tails such that the animals can move about freely in their cage and access food and water but cannot

load their hindlimbs⁴⁹. This model in mice and rats consistently induces bone loss in the hindlimbs similar to that which would be seen in other mechanical unloading methods. Young rats who undergo tail suspension experience decreases of 20-50% of trabecular bone volume in the distal femur and proximal tibia after 14 days of tail suspension^{50,51}. Cortical bone decreases of 5-10% have been reported in tail suspended rats who are suspended for periods of 28 days or longer^{52,53}. Tail suspension studies in mice demonstrate trabecular bone volume losses of 20-30% after 14 days of unloading in the distal femur and proximal tibia^{54,55} and losses rise to 30-50% of trabecular bone volume in the distal femur and proximal tibia after 28 days of unloading^{56,57}. Cortical bone loss in tail suspended mice is smaller in magnitude but studies have found a 4-6% decrease in cortical thickness after 14 days of tail suspension⁵⁸ and a 6-10% decrease in cortical thickness after 28 days of tail suspension⁵⁶. Bone loss in mice in response to tail suspension can be dependent on the genetic mouse strain used, with magnitude of bone loss in response to tail suspension differing between the bones of several genetic strains of mice^{54,58,59}. The C57Bl/6J strain of mice and the BALB/c strain of mice are two of the most commonly used mouse strains in tail suspension studies examining bone adaptation due to the large bone loss that these mouse strains consistently exhibit during tail suspension⁵⁹⁻⁶¹.

1.6 Role of osteocytes in disuse-induced bone loss

The mechanisms of disuse-induced bone loss are not fully understood, though a few possible mechanisms have been proposed and investigated. As osteocytes are a regulator of bone resorption through activation of osteoclasts by RANKL, it has been

proposed that osteocytes play a significant role in disuse-induced bone loss. In investigating the role of osteocytes during unloading, a tail suspension study in mice found that during tail suspension, osteocyte apoptosis significantly increased within three days of unloading. In addition, increased osteocyte apoptosis occurred prior to measurable decreases in bone volume⁶⁰. Additional studies confirmed an increase in osteocyte apoptosis during unloading⁶²⁻⁶⁵.

In studies examining fatigue-based loading in bone, osteocyte apoptosis increased the release of pro-osteoclastic signaling molecules from surrounding non-apoptotic osteocytes which would initiate remodeling of the bone surrounding the apoptotic osteocytes^{62,63}. Attempts to determine if osteocyte apoptosis is necessary to disuse-induced bone loss and have found mixed results. In one study by Cabahug-Zuckerman et al., inhibiting osteocyte apoptosis through injections of the pan-caspase inhibitor quinolyl-valyl-O-methylaspartyl-methyl-ketone (QVD) during tail suspension in mice blocked bone resorption⁶⁴. In this study, QVD injections reduce osteocyte apoptosis during tail suspension to the same level as ambulatory control mice. However, in another study by Plotkin et al., inhibiting osteocyte apoptosis through injections of the bisphosphonate alendronate and the bisphosphonate analog IG9402 during tail suspension prevented RANKL release from other osteocytes but bone loss still occurred during tail suspension indicating that RANKL from osteocytes may not be the only signal inducing bone loss in disuse⁶⁵. In this study, they find that alendronate does also inhibit osteoclastic bone resorption while the bisphosphonate analog IG9402 does not. Both treatments reduced osteocyte apoptosis during tail suspension to control levels of normal

ambulatory control mice⁶⁵. As these two studies use different methods for inhibiting osteocyte apoptosis, it is possible that the different responses observed are in part due to methodology. As there is no clear consensus from previous studies, the specific impacts of osteocytes and osteocyte apoptosis during disuse is not yet clear and will require more research to determine.

1.7 Bone recovery during reloading following disuse

While the effect of disuse on bone has been well documented, there are far fewer studies that have tracked the recovery of bone following a period of disuse. A return to normal mechanical loading in bone, or reloading, results in bone slowly returning to its pre-unloaded condition. The specific length of time of full recovery of bone is unclear and depends on what parameters are tracked in recovery. One previous study estimates that recovery can take twice the period of unloading to fully recover bone structure losses during disuse⁵². Other studies demonstrate that some effects of disuse such as reduction of osteoblast number and decreased BMD at multiple skeletal sites, including the femoral neck and lumbar spine, persist and require longer than twice the unloading period to recover^{38,50,66}.

Some spaceflight and bed rest studies have monitored study participants after the disuse period to monitor recovery and in these studies, effects of disuse are still present after twice the unloaded period. In a spaceflight study that monitored astronauts for 1 year following 4-6 month spaceflight bouts, femoral bone mass mostly recovered within

1 year, though BMD and estimated bone strength remained 15-20% lower than pre-spaceflight calculations⁶⁶. In a bed rest study that monitored bone recovery 6 months after a 17 week bed rest, recovery of BMD was present in all areas measured including femoral neck, lumbar spine and tibia, though BMD at all of these locations was still 1-5% lower than pre-bed rest values³⁸.

In rat tail suspension studies, trabecular bone parameters that decreased during unloading tended to return to control levels after a recovery period that had double the duration of the unloading period^{50,67,68}. However, the convention of a recovery period that is twice the unloading period may only allow for recovery of structural parameters in rats, as another study found that volumetric BMD in the proximal tibias of rats that were tail suspended for 28 days did not recover to baseline levels until 84 days of recovery, three times as long as the unloading period⁶⁹. Regardless of potential lingering effects, an unloaded animal that has been allowed a recovery time of twice the unloading time is not more susceptible to additional disuse-induced bone loss in young animals. In a previous study, when unloaded young animals were allowed a recovery time of twice the unloading time, a second identical duration of unloading did not result in more bone loss than during the first bout of unloading⁵². Adding moderate exercise during the recovery time in rats did allow for slightly more rapid bone recovery, but this did not protect against bone loss during a second unloading period⁶⁷.

Bone adaptation during early reloading is also not well characterized and the timeline during which unloading-induced bone loss stops and bone recovery begins during reloading is unknown. In a spaceflight study in mice, after a 30 day spaceflight, the weight-bearing ankle bones experienced further bone loss of 8-10% after 8 days of reambulation in normal gravity⁴¹. Another study found that the tibia, femur and spine of mice who had taken a 30 day spaceflight had not begun to recover bone that had been lost by 8 days after return to earth⁴⁴. Further studies are needed to establish whether bone loss during early reloading is the expected result. It may be the case that early periods of increased loading following a period of mechanical unloading may be a vulnerable time for bone in which fracture risk may be increased due to bone loss.

1.8 Aging and bone

Humans achieve peak bone mass in their 20s or 30s, after which bone mass stays relatively stable for a couple of decades which begins to decrease with advancing age^{8,70,71}. Women experience a rapid decrease in bone mass for a period following menopause, and then experience a slower consistent decrease thereafter^{8,72,73}. Meanwhile, men experience a consistent decrease in bone mass of similar magnitude as that of women as they age without being susceptible to the rapid bone loss associated with menopause^{8,72}. This age-related loss in bone mass is associated with characteristic changes in bone structure. Cortical porosity in long bones increases with age⁷⁴, and trabecular thickness and trabecular number decrease in trabecular bone⁷⁵⁻⁷⁸. Trabecular bone loss with age occurs at most sites of trabecular bone, in the vertebral bodies of the spine^{77,78} and in the metaphyses and epiphyses of the long bones^{75,76,79}. Long bones also

experience cortical thinning due to bone resorption on the endosteal surface. To counteract the decreased mechanical strength that comes with cortical thinning, new bone is formed on the periosteal surface, resulting in an overall increase in the outer diameter of the bone due to periosteal expansion⁸⁰.

Within the bone tissue, age results in many changes to the bone mineral and collagen matrix. In the collagen matrix, collagen stability within bone decreases with age⁸¹, enzymatic collagen crosslinks within bone decrease while non-enzymatic collagen crosslinks increase⁸². In addition, the mineral-to-matrix ratio of bone increases with age, which increases the crystallinity of the bone^{8,83}. This can cause the bone tissue to become stiffer, but more brittle. While many of these changes reflect a decrease in bone mass with age, many also reflect a decrease in bone quality⁸³. Bone quality is an overarching term encompassing all factors outside of bone quantity that affect bone mechanical properties, including the bone's geometry and microstructure, porosity, accrued damage, mineralization, mineral and collagen properties.

Aging also affects osteoclasts, osteoblasts and osteocytes, which directly affects the mechanisms of bone turnover⁷¹. Studies in humans that isolated bone marrow cells from participants of a variety of ages found that osteoclastogenesis increases with age^{71,84}. Increased osteoclastogenesis contributes to the imbalance between bone resorption and bone formation in older subjects that contributes to steady bone loss with age and the development of osteoporosis. The vast majority (60-90%) of osteoblasts that

form bone during bone remodeling undergo apoptosis at the termination of bone remodeling⁸⁵ and this rate of osteoblast apoptosis may increase age^{86,87}. In addition, several studies have reported that osteoblast differentiation from osteoblast precursors is diminished with age^{87,88}, which may contribute to decreased bone formation in older subjects⁸⁹. It is well documented that osteocyte density in bone also diminishes with age⁹⁰⁻⁹², and osteocyte apoptosis increases with age⁹³, leaving empty lacunae that may become hypermineralized in rodents^{71,94} but not in humans. A reduction in osteocyte density can impair the bone's ability to properly sense mechanical loads, reducing bone remodeling in response to microdamage, and leading to the accumulation of microdamage⁹⁵.

Aging also causes additional changes in systems that can impact bone turnover. It is well documented that elderly patients experience a higher basal inflammatory environment that could contribute to changes in bone formation and resorption⁹⁶⁻⁹⁸. In addition, circulating inflammatory biomarkers are higher in older subjects than younger subjects at a basal level^{80,99}. It is also suggested that macrophages might be less responsive to the same inflammatory signal in older subjects¹⁰⁰. The cytokines produced and released by macrophages can have major effects on the activation and activity of osteoclasts. Thus, changes in these factors with age could affect bone turnover in older subjects.

1.9 Disuse in aged bone

Though bone adaptation in adult subjects in response to disuse is well documented^{32,37,45,50,52}, very little research has examined the response of bones of aged subjects. Previous studies have examined young or adult subjects; participants in human bed rest studies are typically 25-40 years old^{32,33}, astronauts in spaceflight studies have an average age of 40-45 years old^{36,101,102}, and animal studies typically use skeletally mature animals, 12-16 weeks old in mice and 4-6 months old in rats^{52,53}. Human bed rest studies are typically considered to be a higher risk for older subjects and are not performed on older subjects.

Studies that have examined disuse in older animals are limited but indicate that there may be key differences in the magnitude and timeline of bone adaptation to disuse in older animals. A tail suspension study using young and old rats found that old rats did not experience any decrease in trabecular bone parameters, but did experience increased cortical bone porosity following two weeks of unloading whereas young rats experienced a significant decrease in trabecular bone parameters but did not experience any cortical bone changes¹⁰³. However, a second study examining only old rats found that two weeks of tail suspension resulted in lower trabecular bone parameters in the femur and tibia compared to old rats that had been allowed normal ambulation¹⁰⁴. The lack of studies examining bone adaptation to disuse in older animals makes it difficult to fully understand the differences between the skeletal response in old subjects compared to young subjects. Importantly, none of these previous studies examined a recovery

period following disuse in aged subjects, and thus any age-related differences in the skeletal response to reloading is completely unknown.

1.10 Summary and knowledge gap

The adaptation of bone in response to disuse is well established in young subjects. However, the adaptation of bone during unloading in older subjects is less well characterized and requires more research. Disuse-induced bone loss during a period of immobility such as an injury or hospitalization is a pressing health concern in older patients. While there is some evidence that bone loss during disuse might be impaired in older subjects¹⁰³, there are too few studies examining old subjects to fully characterize the difference in bone adaptation response. In addition, recovery of bone following disuse has not been studied in old subjects. Even in young subjects, recovery from unloading-induced bone loss happens on a much longer timeline than the bone loss itself, and it is possible that there is a period of continued bone loss during early reloading prior to reversal to a bone formation phase. If there is a significant period of bone loss even after the start of reloading in young subjects, this period could potentially be even longer in older subjects, as it is established that bone adaptation to increased loading is impaired in old subjects.

In this research, we aimed to characterize bone adaptation of old and young subjects in response to mechanical unloading and subsequent reloading. We used a tail suspension model in rats and mice as the mechanical unloading stimulus. In mice we

compared this bone adaptation in young and old mice to a transgenic mouse model with decreased osteocyte density to attempt to describe the effect of osteocyte density on bone adaptation in response to unloading and subsequent reloading. This research will expand our understanding of age-related changes in bone adaptation and may provide valuable insights into treatments to protect skeletal health in the elderly.

Chapter 2: Age-Dependent Recovery of Bone During Reloading Following a Period of Hindlimb Unloading in Rats

Hailey C. Cunningham, Daniel W.D. West, Leslie M. Baehr, Franklin D. Tarke, Keith Baar, Sue C. Bodine, Blaine A. Christiansen

2.1 Abstract

Background: Bone structure and strength are rapidly lost during conditions of decreased mechanical loading, and aged bones have a diminished ability to adapt to increased mechanical loading. This is a concern for older patients that experience periods of limited mobility or bed rest, but the acute effects of disuse on the bones of aged patients have not been thoroughly described. Previous animal studies have primarily examined the effect of mechanical unloading on young animals. Those that have studied aged animals have exclusively focused on bone loss during unloading and not bone recovery during subsequent reloading. In this study, we investigated the effect of decreased mechanical loading and subsequent reloading on bone using a hindlimb unloading model in Adult (9-month-old) and Aged (28-month-old) male rats.

Methods: Animals from both age groups were subjected to 14 days of hindlimb unloading followed by up to 7 days of reloading. Additional Aged rats were subjected to 7 days of forced treadmill exercise during reloading or a total of 28 days of reloading. Trabecular and cortical bone structure of the femur were quantified using ex vivo micro-computed tomography (μ CT), and mechanical properties were quantified with mechanical testing.

Results: We found that Adult rats had substantially decreased trabecular bone volume fraction (BV/TV) following unloading (- 27%) while Aged animals did not exhibit significant bone loss following unloading. However, Aged animals had lower trabecular BV/TV after 3 days of reloading (- 20% compared to baseline), while trabecular BV/TV of Adult rats was not different from baseline values after 3 days of reloading. Trabecular BV/TV of Aged animals remained lower than control animals even with exercise during 7 days of reloading and after 28 days of reloading.

Conclusions: These data suggest that aged bone is less responsive to both increased and decreased mechanical loading, and that acute periods of disuse may leave older subjects with a long-term deficit in trabecular bone mass. These findings indicate the need for therapeutic strategies to improve the skeletal health of elderly patients during periods of disuse.

2.2 Background

Bone undergoes a significant and rapid decay in structure and strength in the absence of mechanical loading^{49,72,105}. In addition, bones of aged humans and animals have a diminished ability to adapt to the mechanical loading environment^{106,107}, making exercise or increased mechanical loading less effective at building bone mass. This is particularly important, as older patients commonly experience periods of limited mobility or skeletal unloading during periods of sickness or following an injury or surgery, and the ability to regain bone mass following a period of unloading may be compromised.

The effect of mechanical unloading on bone has been extensively studied in both humans and animal models. In humans, a prolonged period of unloading decreases bone volume and bone density as illustrated through bed rest and spaceflight studies^{101,105,108}. For example, women who participated in 60 day bed rest had decreases of 3-4% in bone mineral density in the trabecular bone of the femur and tibia³⁷. Similarly, astronauts who spent prolonged time in space experienced a 1-2% trabecular bone mineral density loss in the hip and spine per month in space¹⁰². Similarly, early models of unloading in mice and rats, including spaceflight studies and tail suspension, found that trabecular and cortical bone volume are rapidly lost during periods of disuse^{34,50,52,103,105}. Losses of 20-50% of trabecular bone volume in the proximal tibia have been reported after two weeks of hindlimb unloading in adult rats^{50,51}. In addition, longer bouts of unloading of 28 days have resulted in small (~5%) decreases in cortical bone mineral density^{52,53}. While the effect of mechanical unloading on bone has been thoroughly investigated, there have been relatively few studies examining the structural recovery of bone during reloading, and the factors that affect this recovery. Previous studies indicate that full recovery of bone mineral density requires a reloading period of twice the unloading period^{52,109}. In addition, it has been observed in rats that while bone volume returns to control levels during reloading, the bones still have fewer osteoblasts and a lower bone formation rate⁵⁰.

The effect of mechanical unloading on aged bone is not well established in either humans or animal models. Human spaceflight studies most often involve healthy young males^{101,108}, and there are few bed rest studies using older patients, most of which have investigated the effect on muscle rather than bone^{110,111}. In animal models, few studies

have investigated the role of age in bone adaptation to unloading, and the effect of age on the reloading response has not been investigated¹⁰³. Most prior rodent studies have either used young developing animals (5-7 weeks old in the case of rat studies)^{50,105,112} or young adult animals (4-6 months old in the case of rat studies)^{52,53,113}. It has been suggested that bone of aged rats does not respond at all to short bouts of unloading¹⁰³ however there has been no examination of aged animals during reloading to examine any delayed effects of unloading. It is therefore unknown to what degree aged bone exhibits an adaptive response to mechanical unloading, and to what extent aged bone is able to recover from unload-induced bone loss during reloading.

In the current study, we used hindlimb unloading and subsequent reloading of skeletally mature Adult and Aged rats to examine the effect of age on bone loss during mechanical unloading and bone recovery during mechanical reloading. Rats underwent hindlimb unloading for 14 days; this unloading duration has been shown to cause a significant loss of trabecular bone in Adult animals^{50,52}, and this unloading period was previously used to examine bone loss in Aged rats¹⁰³. Cortical and trabecular bone structure was assessed using micro-computed tomography. Three-point bending and trabecular bone compression mechanical testing were used to assess changes in structural and mechanical properties. We hypothesized that Adult rats would exhibit considerable bone loss during unloading, while Aged rats would exhibit less or no significant bone loss as was observed in a past study¹⁰³. We further hypothesized that Adult rats would fully recover bone during reloading, while any bone loss observed following unloading in Aged rats would not be fully recovered during the reloading period.

The results of this study could inform interventions such as exercise or mechanical loading for bone fragility in older subjects, particularly in the context of periods of mechanical disuse.

2.3 Methods

2.3.1 Animals

This study used a total of 63 Fisher 344 x Brown-Norway (FBN-F1) male rats from the National Institute of Aging (NIA) Aged Rodent Colony (Charles River Laboratories, Wilmington, MA). Rats were either 9 months old (“Adult”, n = 23), or 28 months old (“Aged”, n = 40). All rats were housed individually. Rats were cared for in accordance with the guidelines set by the National Institutes of Health (NIH) on the care and use of laboratory animals. All procedures were approved by the Institutional Animal Care and Use Committee at UC Davis.

2.3.2 Experimental groups and study design

Eleven experimental groups (n = 5–6 rats per group) were used to determine the magnitude of bone loss during hindlimb unloading and bone recovery during reloading (Fig. 2.1). Baseline animals (5 Adult and 6 Aged) were euthanized prior to unloading to determine bone structure before intervention. The remaining rats underwent 14 days of hindlimb unloading via tail suspension. Post-unloading, one group of animals (6 Adult and 5 Aged) was euthanized immediately. Remaining rats were removed from hindlimb

suspension and allowed to return to normal cage activity for 3 days (6 Adult and 6 Aged) or 7 days (6 Adult and 6 Aged). Additional groups of Aged rats examined the effect of activity level during reloading, and the effect of longer-term reloading. A group of Aged rats (n = 6) underwent 14 days of hindlimb unloading followed by 7 days of reloading with daily treadmill walking (an average of 13.8 m/day) to account for a significant decrease in activity observed in this age group during the first 5 days of reloading. Rats were set to walk on the treadmill at a quick walk (73 m/min) until they had covered the decrease in distance between the rats before and after unloading. Another group of Aged rats (n = 5) underwent 14 days of hindlimb unloading followed by 28 days of normal cage activity. To account for age-related decrease in bone, an additional group of Aged rats (n = 6) that were not subjected to hindlimb unloading were used as an age-match control to the 28 days reloaded group.

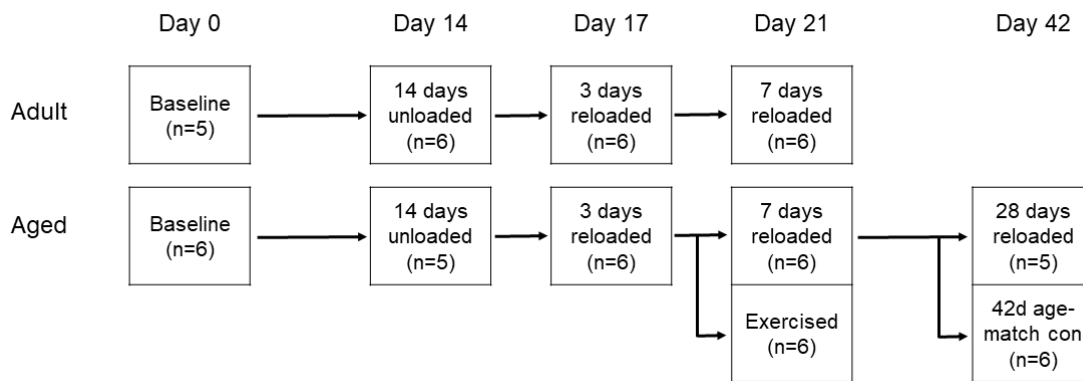


Figure 2.1: Experimental design. Adult (9-month-old) and Aged (28-month-old) rats (n = 63) were used for this study. Baseline rats were euthanized at day 0. Remaining groups underwent 14 days of hindlimb unloading, with a group of rats euthanized immediately following hindlimb unloading. All remaining rats were returned to normal cage activity. Rats from both age groups were euthanized after 3 or 7 days of reloading. An additional group of Aged rats were euthanized after 7 days of reloading with timed treadmill walking for the first 5 days of reloading. Two additional groups of Aged rats were euthanized after 28 days of reloading or at an equivalent age for age-match control (not subjected to hindlimb unloading).

2.3.3 Hindlimb unloading via tail suspension

Rats were subjected to hindlimb unloading via tail suspension as originally described by Morey-Holten⁴⁹. Briefly, the skin of the tail was cleaned using an alcohol pad, dried, and then sprayed with a light coating of tincture of benzoin. A tail-wide strip of Skin-Trac was then looped around a metal bar and applied to two sides of the tail. The tail was wrapped with Medi-Rip LF self-adherence bandage and then the animal was suspended by attaching the metal bar to a swivel hook above the suspension cage. The height of the hook was adjusted so that only the front limbs were able to touch the bottom of the cage. The rats were able to freely rotate in all directions within their cage and had free access to food and water. Body weights of the rats were taken prior to suspension and monitored throughout the unloading period. Following unloading or reloading, the rats were euthanized and their hindlimbs collected and stored in 70% ethanol prior to analysis. Previous studies have shown that storing bones in ethanol has little effect on the mechanical properties of the bone if properly rehydrated before testing^{114,115}.

2.3.4 Cage activity

Prior to unloading and during reloading, cage activity of Adult and Aged rats was measured using the Home Cage Photobeam Activity System (San Diego Instruments). Each rat was housed individually, and activity was tracked throughout the 12-h dark cycle and for the first hour of the light cycle. Data was analyzed using the Photobeam Activity System software.

2.3.5 Micro-computed tomography analysis of trabecular and cortical bone

Femurs were scanned with micro-computed tomography (μ CT 35, Brüttsellen, Switzerland) to analyze morphological changes in trabecular and cortical bone during unloading and reloading. Bones were scanned with x-ray tube potential 55 kVp, intensity 114 mA, integration time 900 ms, 15 μ m isotropic nominal voxel size. Trabecular bone analysis was performed at the distal femoral metaphysis over a region of 200 slices (3 mm), starting immediately adjacent to the distal femoral growth plate. Trabecular bone volume fraction (BV/TV), trabecular number (Tb.N), trabecular thickness (Tb.Th), trabecular separation (Tb.Sp), and other structural parameters were calculated using the manufacturer's 3D analysis software. Cortical bone was analyzed with 200 slice (3 mm) volumes of interest, centered at 25, 50, and 75% of the length of the diaphysis. Bone area (B.Ar), total cross-sectional area (T.Ar), cortical thickness (C.Th), maximum and minimum moments of inertia (I_{\max} and I_{\min}), and other structural parameters were calculated using the manufacturer's 3D analysis software.

2.3.6 Three-point bending mechanical testing

Following μ CT imaging, femurs were mechanically tested in three-point bending using a materials testing system (ELF 3200, TA Instruments, New Castle, Delaware) to determine cortical bone structural and mechanical properties. Femurs were immersed in phosphate-buffered saline for at least 10 min prior to testing to rehydrate the bone tissue in an isotonic solution. The midpoint of each femur was measured and marked, and each sample was placed in the 3-point bending setup such that the midpoint of the bone was

directly under the loading platen. The two lower platens were 13 mm apart, and bones were tested with the caudal aspect of the bone in tension. A single monotonic load to fracture was applied at a slow (quasi-static) loading rate of 1 N/sec. Force and displacement data were recorded at 100 Hz. From the resulting force-displacement data, the yield point was visually identified as the point at which the linear portion of the curve ended. Bending stiffness (K), yield force (F_y) and ultimate force (F_{ult}) were determined from this data. Bone geometry determined from the μ CT scan was used to calculate bending modulus (E), yield stress, and ultimate stress.

2.3.7 Metaphysis trabecular bone compression

After testing with 3-point bending, trabecular bone of distal femurs was mechanically tested in compression as described by Hogan et al.¹¹⁶. Distal femurs were potted in bone cement in a small petri dish to hold the bones stationary. Approximate location of the growth plate (determined from the μ CT images) was marked on the outer surface of the femur. A 3 mm thick slice of the femoral metaphysis was then cut from the region adjacent to the growth plate, including both cortical and trabecular bone. Compression testing was performed with a materials testing machine (ELF 3200, TA Instruments, New Castle, DE). Samples were rehydrated in phosphate-buffered saline for at least 10 min prior to mechanical testing. The bone slice was loaded between two circular platens with diameter of 3 mm such that the platens were only in contact with the trabecular bone and not the cortical bone. Following a preload of 1–2 N, a monotonic (quasi-static) load was applied to the slice at a rate of 0.005 mm/sec. Compression continued to a target displacement of 0.2 mm. Force and displacement data was recorded

at a rate of 100 Hz for the duration of the test. From this data, yield and ultimate force, yield and ultimate displacement and stiffness were obtained. Effective stress and effective modulus were obtained by normalizing by the surface area of the platens.

2.3.8 Statistical analysis

Differences in body weight and cage activity before and after unloading in Adult and Aged animals were analyzed by paired Student's t-test. The majority of statistical analyses were performed using 2-way analysis of variance (ANOVA) stratified by age and experimental group for main effect, with post-hoc analysis using Tukey's test. Statistical significance was defined as $p < 0.05$. The additional Aged rat group (7 days reloaded with treadmill walking) was analyzed for significance against the Aged baseline group and Aged 7 days reloaded group with a 1-way ANOVA stratified by experimental group with statistical significance defined as $p < 0.05$. The additional Aged rat groups of 28 days reloaded and 28 days age-matched control were analyzed for significance against the baseline group with a 1-way ANOVA stratified by experimental group with statistical significance defined as $p < 0.05$. For the trabecular bone compression test, a linear correlation between trabecular BV/TV and the effective elastic modulus and the correlation coefficient for the correlation was obtained.

2.4 Results

2.4.1 Animals

Over 14 days of unloading both age groups of rats experienced a significant decrease in body weight. Adult rats lost 12.2% of their body weight on average and Aged rats lost an average of 14.6% of their body weight¹¹⁷. Cage activity measurements indicated a significant decrease in distance traveled of an average of 13.8 m/day in the first 5 days of reloading compared to baseline levels in Aged rats¹¹⁷; Adult rats exhibited no statistically significant decrease in activity during reloading.

2.4.2 Micro-computed tomography analysis of trabecular bone

At baseline, bones from Aged rats had significantly less trabecular bone volume fraction than those from Adult rats (0.169 vs. 0.247 BV/TV). Bones from Aged rats also had significantly lower Tb.N and higher Tb.Sp than Adult rats at baseline (Fig. 2.2). Trabecular thickness at baseline was not different between the two groups. After 14 days of hindlimb unloading, significant differences from baseline were observed in Adult rats but not Aged rats. Bones from Adult rats had 26.6% lower BV/TV ($p = 0.0493$) after 14 days of unloading compared to baseline. In addition, we observed trends toward decreased Tb.N and increased Tb.Sp at this time point, although these were not statistically significant.

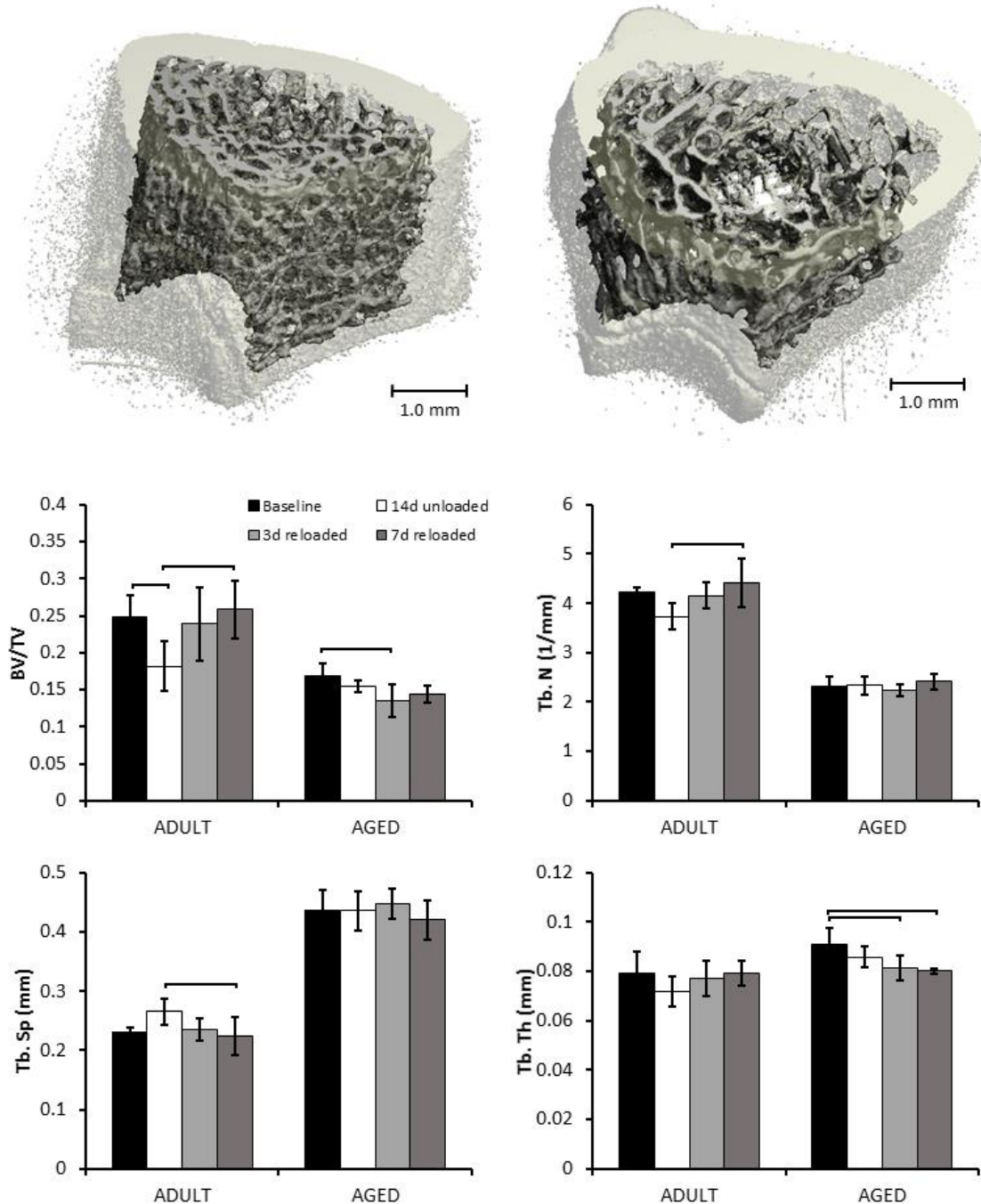


Figure 2.2: Distal femoral metaphysis trabecular μ CT results. Representative regions of interest of trabecular bone for Adult (left) and Aged (right) femurs at baseline. Adult rats exhibited greater BV/TV, Tb.N, and lower Tb.Sp than Aged rats. 14 days of hindlimb unloading resulted in significant loss of trabecular bone in Adult rats, but no significant decrease in Aged rats. By day 3 of reloading, Adult rats had recovered trabecular bone volume, while Aged rats exhibited loss of bone. Data are presented as means and standard deviations. Brackets indicate significant differences between groups ($p < 0.05$).

After 3 days of reloading, trabecular bone parameters of Adult rats were not different from baseline values. In contrast, Aged bones had 19.7% lower BV/TV than baseline values (0.136 vs. 0.169), and 12.0% lower Tb.Th ($p = 0.0096$) at this time point. After 7 days of reloading, trabecular bone parameters of Adult bones were not different from baseline values, while trabecular thickness in Aged rats remained significantly lower than baseline values.

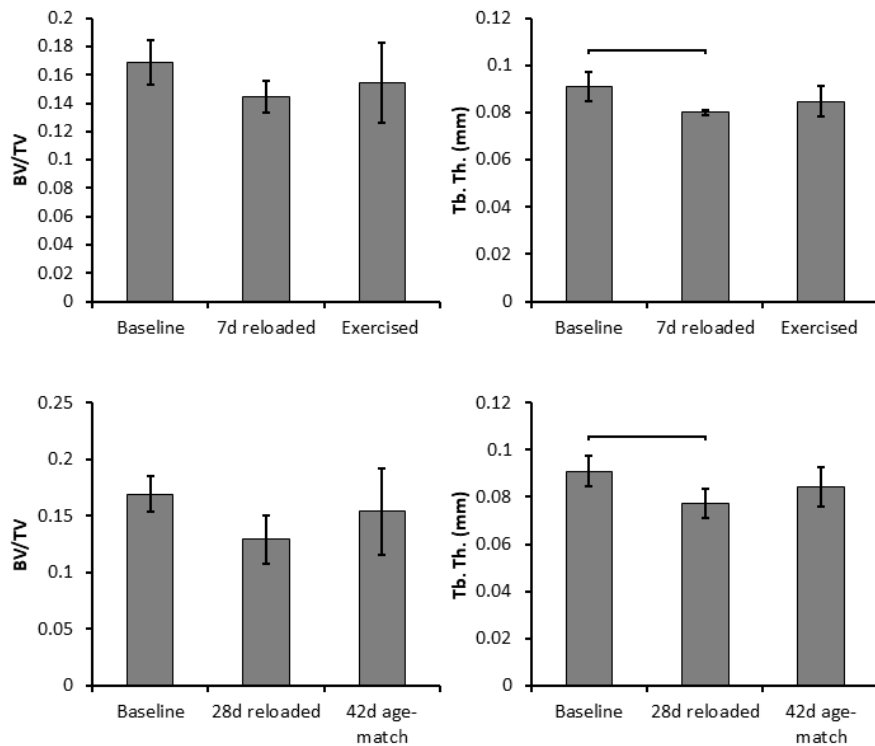


Figure 2.3: Metaphyseal trabecular bone structure of (top) 7 days reloaded and 7 days reloaded with exercise and (bottom) 28 days reloaded Aged and 42 day age matched Control rats. 7 days of treadmill walking during reloading did not significantly increase trabecular bone parameters relative to the 7 days reloaded group. Reloading for 28 days did not restore trabecular thickness back to control levels. Data are presented as means and standard deviations. Brackets indicate significant differences between groups ($p < 0.05$).

Aged rats subjected to 14 days of unloading followed by 28 days of reloading, had 15.1% lower Tb.Th than baseline ($p = 0.0068$), and 8.2% lower Tb.Th than the age-matched control group, though this difference was not statistically significant (Fig. 2.3). Trabecular BV/TV was not significantly different from baseline values after 28 days of reloading.

Seven days of treadmill walking during reloading in Aged rats did not significantly increase trabecular bone parameters compared to the 7 days reloaded group. BV/TV was 6.8% higher and Tb.Th was 5.9% higher in the exercised group than in the 7 days reloaded group, but these increases were not statistically significant.

2.4.3 Micro-computed tomography analysis of cortical bone

Significant differences in cortical bone structure were observed between Adult and Aged rats, however few differences were observed within either age group due to unloading or reloading. Aged rats had significantly lower cortical thickness and significantly higher bone area and total area than Adult rats (Fig. 2.4). I_{max} and I_{min} were also significantly higher in Aged rats than Adult rats. These observations were consistent across all three regions analyzed within the femoral diaphysis.

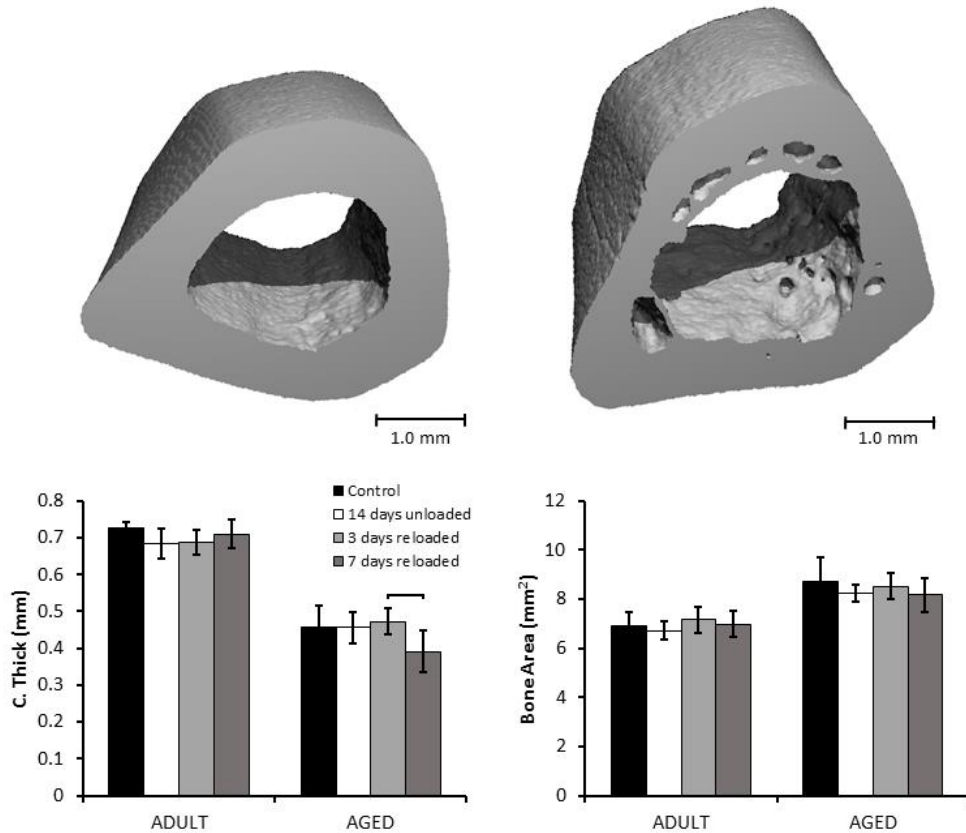


Figure 2.4: Mid-femoral diaphysis cortical μ CT results. Representative samples of regions of interest in Adult (left) and Aged (right) femurs. Aged rats had lower average cortical thickness than Adult rats, but greater bone area and total cross-sectional area. Neither age group exhibited changes in cortical structure due to hindlimb unloading or reloading. Brackets indicate significant differences between groups within Adult or Aged rats ($p < 0.05$).

2.4.4 Three-point bending mechanical testing

3-point bending yielded similar results to the μ CT analysis of cortical bone, with Aged bones generally exhibiting greater structural properties and lower material properties than Adult bones (Fig. 2.5), but no significant differences within either age group due to hindlimb unloading or reloading. Stiffness and ultimate force were 34.7% higher ($p < 0.0001$) and 11.5% higher ($p < 0.001$) in Aged rats than the Adult rats at

baseline, respectively. Yield stress was 39.1% lower ($p < 0.0001$) in Aged rats compared to Adult rats, while ultimate stress similarly was 28.8% lower ($p < 0.0001$) in Aged rats. Elastic modulus was 25.1% lower ($p < 0.0001$) in Aged rats than Adult rats.

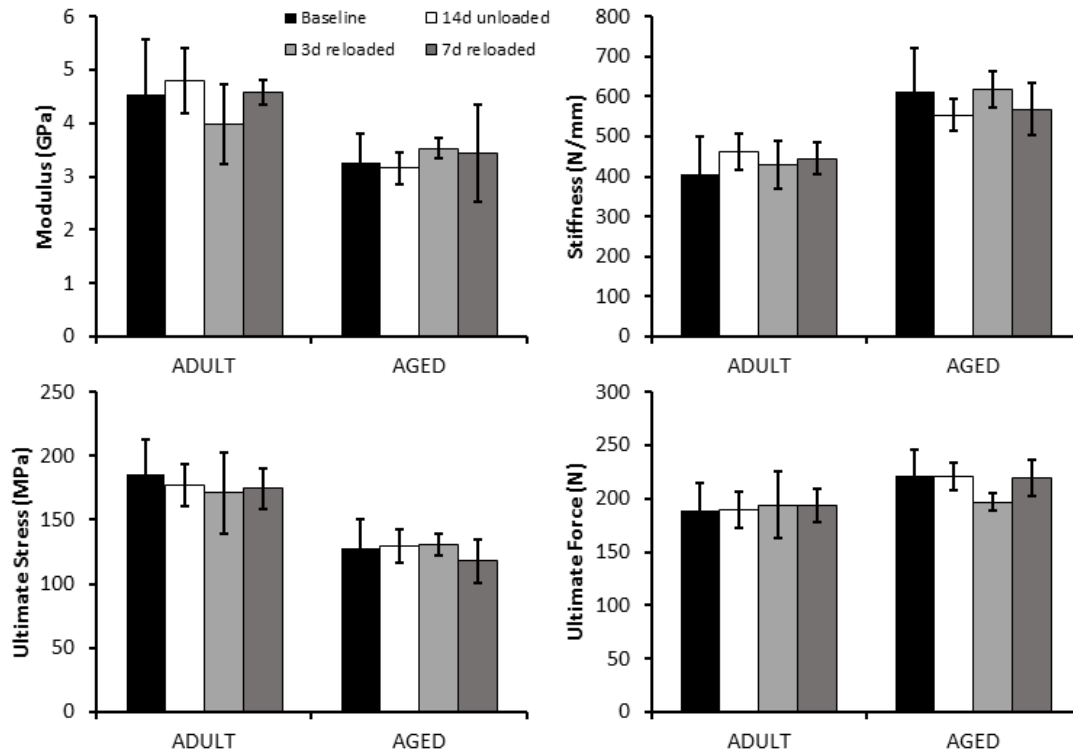


Figure 2.5: Three-Point bending results. Bones from Aged rats exhibited greater stiffness and ultimate force, but lower bending modulus and ultimate stress compared to bones from Adult rats. Data are presented as means and standard deviations. No significant differences were observed as a result of hindlimb unloading or reloading.

2.4.5 Trabecular bone compression

Trabecular bone compression yielded trends similar to results of the trabecular bone μ CT analysis. However, only age-related differences achieved statistical significance (Fig. 2.6). Trabecular bone from Adult rats exhibited significantly higher stiffness (+ 82.5%), effective modulus (+ 82.5%), and effective yield stress (+ 146.5%)

than those from Aged rats. In the 14 days unloaded Adult rats, we observed trends towards lower stiffness, effective modulus, and effective yield stress compared to baseline values. However, these differences were not statistically significant due to the high variance in the experimental groups. The correlation between BV/TV and effective modulus yielded a correlation coefficient of 0.758, indicating a high correlation between these variables that was statistically significant ($p < 0.0001$) (Fig. 2.6).

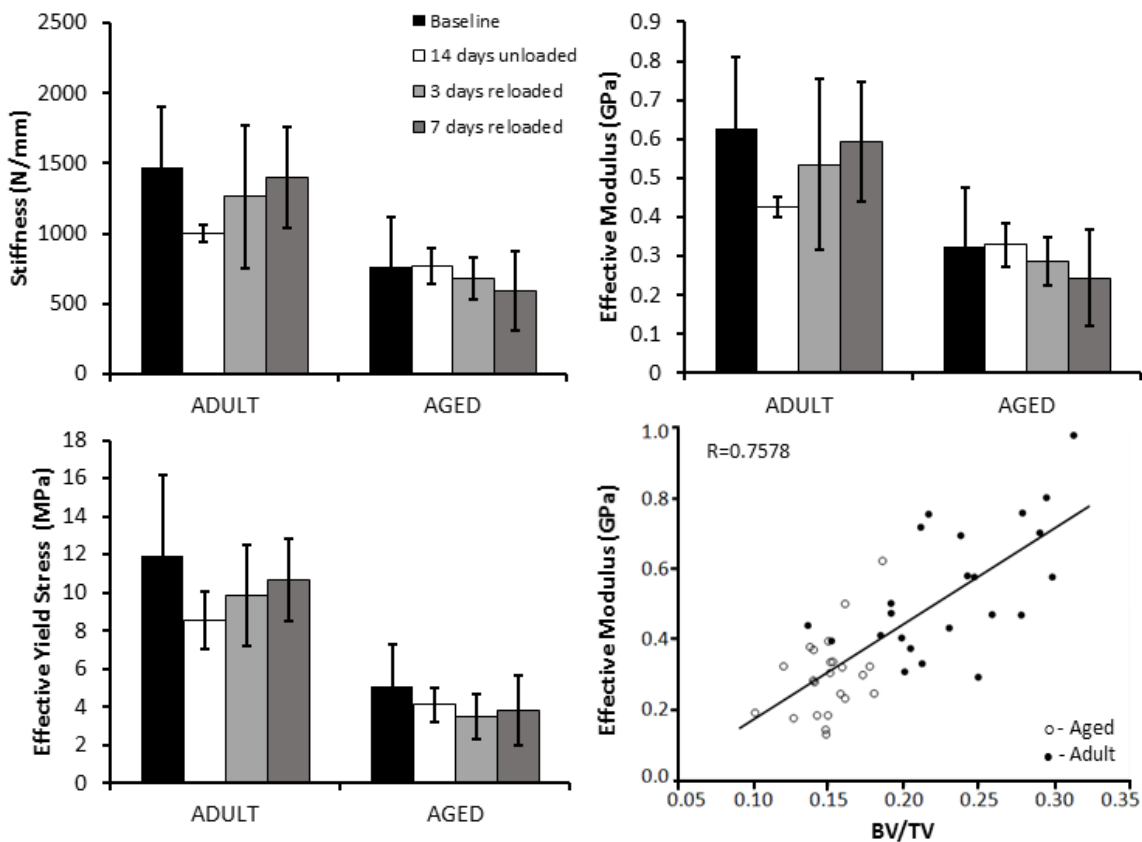


Figure 2.6: Trabecular bone compression results. Bones from Adult rats exhibited significantly greater stiffness, effective modulus, and effective yield stress than bones from Aged rats. However, there were no significant differences observed as a result of hindlimb unloading or reloading. Data in column graphs are presented as means and standard deviations. Effective modulus showed a strong correlation to BV/TV.

2.5 Discussion

This study investigated differences in bone adaptation to hindlimb unloading and subsequent reloading in Adult and Aged rats. We originally hypothesized that Adult rats would lose more bone compared to Aged animals, and that Aged rats would lose little bone with unloading or even have no apparent bone loss. We also hypothesized that if Aged animals did exhibit bone loss during the unloading period, they would have diminished recovery of bone during reloading. Consistent with this hypothesis, we found that Adult rats showed a marked decrease in trabecular bone volume in response to hindlimb unloading, while Aged rats showed no adaptive response in bone during disuse. However, contrary to what has been postulated in previous studies, this does not mean that the Aged rats were necessarily unaffected by unloading. Aged rats did not lose a significant amount of bone volume during the unloading period but did have lower BV/TV and Tb. Th. than baseline after 3 days and Tb. Th. remained lower at 7 days of reloading. These data suggest that there may be a delay in the adaptation of Aged bone to disuse. Consistent with our initial hypothesis, trabecular bone of Adult rats was not different from baseline levels after 3 days and 7 days of reloading, while bones from Aged rats exhibited some deficits in trabecular microstructure even up to 28 days of reloading. These results may suggest that the Aged bones are overall less able to adapt to both unloading and reloading, and that the adaptive response may be temporally delayed. These results may also be a reflection of age-related changes in bone turnover rates and/or bone cellularity, which could lead to different responses to the same periods of unloading and reloading.

The magnitude of trabecular bone loss we observed in Adult rats during hindlimb unloading was similar to previous studies^{52,53}. Decreases in bone formation biomarkers and increases in bone resorption biomarkers have been observed in bed rest studies^{118,119} while in adult rats, bone formation in the hindlimbs has been shown to slow and ultimately cease after one week of tail suspension¹²⁰. In addition, unloading leads to decreased vascularization in the bone, which could impair remodeling and slow recovery during reloading¹²¹. These are all possible mechanisms for trabecular bone loss observed during unloading in this study, though further studies are needed to confirm these mechanisms.

Few studies have examined the effect of tail suspension on aged animals, and those that have focused solely on unloading with no examination of bone recovery during reloading. One such study found that aged rats are less responsive to unloading and do not lose a significant amount of bone during 14 days of unloading¹⁰³. This is consistent with our observations in this study, in which there was no significant loss of trabecular bone volume during unloading of Aged rats, though a non-significant trend toward bone loss was observed. However, this previous study suggested that aged bone may not respond at all to decreased mechanical stimulation¹⁰³; our current data somewhat contradict these conclusions. While it is true that Aged bones showed no significant decreases in trabecular bone microstructure following the unloading period of our study (14 days), we observed a significant decrease from baseline values in trabecular BV/TV after 3 days of reloading and significant decreases in Tb.Th after 3 and 7 days of

reloading. This implies that rather than aged bones being unresponsive to disuse, they may instead experience a delayed reaction to unloading.

It is possible that the gradual loss of trabecular bone in Aged rats could be partially due to normal age-related decreases in bone mass or diminished activity by Aged rats during the reloading period. To address these potential factors, we included a control group of Aged rats that were age-matched for the 28 days reloaded group, and a group that was subjected to 7 days of treadmill walking during reloading to restore normal activity levels. We discovered that forcing Aged rats to resume a moderate activity level did appear to lessen some of the bone loss at 7 days of reloading but did not account for the entire magnitude of bone loss. This implies that a return to a moderate exercise level following periods of disuse may be beneficial in mitigating bone's delayed reaction to unloading.

In Aged rats there was evidence that some bone recovery eventually occurs during reloading. The 28 days reloaded group had no significant differences in BV/TV from baseline. However, Tb.Th. was still lower than baseline after 28 days of reloading in Aged rats. This decrease may be in part due to natural loss of bone due to aging but cannot fully be explained by this since the age-matched control group had trabecular bone parameters that were not significantly different from either the baseline or the 28 days reloading. These data suggest that even after a long reloading period, Aged rats may still have residual deficits in trabecular bone microstructure.

A previous study by Shirazi-Fard et al. showed that over a long period of reloading (28 days or more) in young adult rats, trabecular bone mineral content eventually returns to baseline levels, with recovery requiring twice the unloading time¹⁰⁹. This is in contrast to what we observed in our study, wherein Adult rats exhibited recovery of trabecular bone volume in a much shorter time frame (3–7 days). It is unclear why these different outcomes were observed. Rats in our study were hindlimb unloaded for 14 days, while the study by Shirazi-Fard used 28 days of hindlimb unloading. This longer period of unloading may have caused biological changes that made it more difficult for trabecular bone to recover during reloading. For example, it has been observed that while bone volume may return to control levels, reloaded bones still have fewer osteoblasts and a lower bone formation rate than control bones⁵⁰, indicating that there are important long-term biological effects of unloading. Our current study did not examine changes in cellular activity in these bones, therefore we cannot determine if osteoblast number or activity were altered. Importantly, our study used a cross-sectional study design, so longitudinal changes are inferred using different groups of rats, rather than tracking the same group of rats over time. In contrast, the study by Shirazi-Fard¹⁰⁹ used both longitudinal assessment of bone structure and cross-sectional bone imaging and mechanical testing. It is difficult to say how accurately the inferred longitudinal changes in our study represent the true magnitudes and timeline of adaptive bone changes.

In this study, we observed that cortical and trabecular bone adapted very differently to changes in the mechanical loading environment. Differences in trabecular bone microstructure were easily detected in Adult rats immediately following unloading and at

early time points during reloading, while Aged rats exhibited differences in trabecular microstructure between baseline at later time points. In contrast, cortical bone did not exhibit any adaptation to changes in loading at any time points. This is consistent with previous studies that have found that hindlimb unloading in rats and mice has an effect on cortical bone only for unloading bouts of longer than 14 days⁵³. Considering the lack of cortical bone adaptation determined by μ CT, it was not surprising that three-point bending showed no changes in mechanical properties as a function of unloading and reloading. In trabecular bone mechanical testing, we anticipated a similar trend to the changes in trabecular bone structural parameters from the μ CT analysis. The high variances in the test resulted in no significant differences between experimental groups, however we were able to demonstrate that the mechanical properties of the trabecular bone were highly correlated to the structural properties found in μ CT analysis.

Though we observed no changes in cortical bone in response to changes in loading, we observed significant age-related differences in structural and material properties between Adult and Aged rats. The structural differences we observed, such as lower Ct.Th and larger I_{min} , and I_{max} in Aged rat bones, are consistent with previous studies in which bones from older animals had larger diameters but thinner cortical shells^{122,123}. During aging, bone resorption increases on the endocortical surface of bone resulting in cortical thinning^{74,124}. In response to this resorption, bone formation increases on the periosteal surface of the bone, increasing the bone's cross-sectional area, in an attempt to preserve some of the bone's mechanical properties⁸⁰. We also observed that stiffness

was higher in Aged animals while modulus and ultimate stress were lower; these data are also consistent with previous studies^{123,125}.

The findings of this study have significant implications for aged patients. During sickness, or following an injury or surgery, older patients may spend a prolonged period in bed rest or with limited movement. Such a period of disuse could result in a loss of bone mass, which has previously been confirmed in human studies^{37,118}. Our data suggests that there may be a delay in the skeletal response to a decrease in mechanical loading, and bone loss may continue even during reloading. Clinically, this delay would be concerning as elderly patients who are remobilizing after bed rest may be more vulnerable to subsequent fracture. Our findings may motivate a rethinking of how elderly patients are treated during bed rest or limited mobility and may imply that simply a return to normal activity levels following a period of disuse may not be enough to fully regain skeletal health.

While this study makes strong conclusions about differences between aged and adult bone in response to unloading and reloading, there are a number of limitations that must be addressed. First, this was a cross-sectional study, and did not examine the same animals at baseline, following unloading, and during reloading. Therefore, longitudinal changes due to unloading and reloading must be inferred based on cross-sectional data from different experimental groups. Second, there were no age-matched controls for either Aged or Adult bones at time periods other than 28d reloaded. Third, we did not directly analyze bone formation or bone resorption rates, or other measures of cellular activity in these rats. Even with this limitation, we were able to determine significant

differences in trabecular bone as a function of unloading and reloading, and differences in both cortical bone and trabecular bone as a function of age. Fourth, the group sizes (5–6 animals per group) were small. As a result of the small group sizes, several biologically meaningful measures did not yield statistically significant results. However, even with limited sample size, we were able to demonstrate differences between how aged and adult bones respond during the unloading-reloading timeline, given the cross-sectional nature of the data. Finally, this study did not examine other factors that could contribute to bone remodeling during unloading and reloading such as changes in food and water consumption, changes in gait, or effects of muscle atrophy on loads applied to the bones by muscles, or microdamage subsequent to reloading.

2.6 Conclusions

This study is one of few studies to examine the effect of age on bone adaptation to mechanical unloading, and the first to examine bone adaptation during subsequent reloading in different age groups. We demonstrate that bones from Aged animals have a delayed and diminished adaptive response to mechanical unloading, and an impaired capacity to recover bone during reloading. The delayed response of Aged bone could have meaningful consequences with respect to fracture risk and skeletal health of elderly patients and should be considered for therapies aimed at preserving bone health during periods of disuse and subsequent remobilization.

2.7 Acknowledgements

Research reported in this publication was supported by the National Institute of Arthritis and Musculoskeletal and Skin Diseases under Award Numbers AG045375, and by the Department of Veterans Affairs under Award Number RX000673. The content is solely the responsibility of the authors and does not necessarily represent the official views of the funding bodies. The funding body was not involved with design, collection, analysis, or interpretation of data, or in the writing of the manuscript. The authors have no conflicts of interest to disclose.

Chapter 3: Differential Bone Adaptation to Mechanical Unloading and Reloading in Young, Old and BCL-2 Transgenic Mice

Hailey C. Cunningham, Deepa K. Murugesh, Allison W. Hsia, Benjamin Osipov, Alice Wong, Gabriela G. Loots, Blaine A. Christiansen

3.1 Abstract

Mechanical unloading causes rapid loss of bone structure and strength that will gradually recover after resuming normal loading. However, it is not well established how this adaptation to unloading and reloading changes with age. Clinically, Elderly patients more prone to musculoskeletal injury and longer periods of bedrest, therefore it is important to understand how periods of disuse will affect overall skeletal health of aged subjects, including overall bone mass, bone mineral density and fracture risk. Bone also undergoes age-related declines in structure and function which include decreased trabecular bone mass, cortical thinning and decrease in osteocyte density, which may impair mechanoresponsiveness of the bone. In this study, we examined bone adaptation in response to unloading *via* tail suspension and subsequent reloading in mice. Specifically, we examined the differences in bone adaptation between young (3-month-old) and old (18-month-old) mice in addition to a transgenic mouse model of diminished osteocyte density (BCL-2 transgenic mice). Mice underwent 14 days of hindlimb unloading followed by up to 14 days of reloading. We analyzed trabecular and cortical bone structure in the femur, mechanical properties of the cortical diaphysis of the femur, osteocyte density and apoptosis in cortical bone and serum levels of inflammatory cytokines. We found that young mice lost small amounts of cortical bone and large amounts of trabecular bone during unloading and early reloading, with near total recovery

of trabecular bone at later time points during reloading. Old mice lost moderate amounts of cortical bone and large amounts of trabecular bone during unloading but had minimal recovery of trabecular bone during reloading and no recovery of cortical bone. In BCL-2 transgenic mice, no cortical bone loss was observed during unloading or reloading, but significant trabecular bone loss occurred during unloading and early reloading, with little to no recovery during the reloading period. No significant differences in circulating inflammatory cytokine levels were observed due to unloading and reloading. These results present a possible period of vulnerability in skeletal health in older subjects following a period of disuse that requires further investigation to better protect skeletal health in elderly patients.

3.2 Introduction

Bone loses strength and structure with age^{8,72,80,83}, and old bone is less mechanoresponsive to both increased and decreased loading^{103,106}. However, there is still only a limited understanding of specific age-related differences in bone's response to disuse and the mechanisms behind these differences. Elderly patients make up a disproportionate amount of hospitalizations, and their length of stay for hospitalizations is longer on average than younger adults^{4,5}. As a result, the reduced activity from a hospitalization could have long-term consequences on the musculoskeletal health of an elderly patient who is hospitalized for an extended amount of time. A more complete understanding of how bone adapts to decreased use with age is therefore critical to protecting the skeletal health of elderly patients.

The effect of disuse on bone in young adult subjects has been well established. In humans, bedrest and spaceflight studies have indicated a gradual loss of bone mineral density (BMD) during periods of reduced loading. In bedrest studies, adult women exhibited a 3-4% decrease in trabecular BMD in the femur and tibia during a 60-day bedrest³⁷. Though the scope of subjects is far narrower, spaceflight studies have indicated similar levels of trabecular bone resorption, estimated 1-2% loss of trabecular bone BMD in the hip per month in microgravity^{32,101}. In tail suspension studies in mice, 25-40% of trabecular bone volume fraction in the femur and tibia is lost over a 14-day period of unloading^{64,68,126}.

Far fewer studies have examined the bone recovery that occurs during reloading following a period of unloading. Previous studies establish that bone recovery during reloading take far than the duration of unloading, up to twice as long as the unloading period^{50,52}. Some studies indicate that even after full recovery of bone quantity measures, the effects on bone quality measures such as BMD, osteoblast number and bone formation rate may take even longer to recover^{36,50,66,109}. However, all of these reloading studies were done in adolescent or young adult populations^{37,67,101}. Therefore, these results may not necessarily translate to older subjects, as changes in bone with age could affect bone adaptation during unloading and subsequent reloading.

Bone loses structure and strength with age. Osteoporosis is a low bone mass phenotype most commonly present in older subjects due to a long-term imbalance of

bone formation and resorption resulting in a steady decline in bone mass^{1,2}. Fracture risk in older patients, particularly in patients with osteoporosis or osteopenia, is far higher than for younger patients^{2,73}. With increasing age, bone becomes more brittle and prone to fracture. Trabecular bone in older patients is lost at an average rate of 3-4% per year and cortical thickness is known to decrease with age as well^{8,127}. Osteocyte density in older humans is anywhere from 30-40% lower than it is in younger patients in their 20s and 30s^{90,95}.

The bones of older subjects are also less able to respond to changing loading environments. In humans, exercise in older patients results in smaller increases in bone mass than in younger patients¹²⁸. Similarly, in animal models increased compression of cortical bone resulted in far less additional bone formation in older animals than in younger animals¹⁰⁶. However, far fewer studies have examined the effect of disuse on the bones of older people or animals. Previous studies in rats, including our own previous study, showed that the bones of older animals do not lose as much bone during unloading as younger animals^{103,129}. In addition, in our previous study we observed that old rats continued to lose bone during reloading, which could imply that the adaptation response to decreased mechanical loading was delayed in the old rats.

As mentioned above, osteocyte density decreases in older subjects. Osteocytes are the major resident cells in bone tissue that sense changes in mechanical loading, therefore a decrease in osteocyte density (as in older subjects) could affect the bone

tissue's ability to adapt to decreasing and increasing loads^{60,130}. Genetic mouse models can be used to investigate the effect of the age-related decrease in osteocyte density without other confounding factors associated with aging. One such genetic model is the BCL-2 transgenic mouse established and described by Moriishi et al.¹³¹. In this transgenic mouse, human B-cell lymphoma 2 (BCL-2) is overexpressed in osteoblasts and osteocytes under the control of the Col1a1(2.3kb) promoter. Osteoblasts in this mouse model have suppressed cell adhesion, spreading, and mobility¹³¹. When these osteoblasts are embedded in the bone matrix and become osteocytes, they have fewer, shorter cell processes, and as a result the osteocytes have a disrupted canalicular network and are unable to obtain proper nutrition and eliminate waste, leading to cell death. By 10 weeks of age in this mouse, approximately 50% of osteocytes are dead and by 16 weeks of age 75% of osteocytes have died^{55,131}. Due to an overexpression of BCL-2 in osteoblasts, this mouse model has been characterized to have a high bone mass phenotype, in the long bones, but not the axial skeleton at 4-weeks-old¹³¹ and at 4-months-old⁵⁵.

In this study, we investigated the differences in bone adaptation to unloading and subsequent reloading between young and old mice. In addition, using young BCL-2 transgenic mice, we were able to compare bone adaptation in this model of osteocyte dysfunction to that of young wild-type mice. We hypothesized that old mice would have a decreased and delayed overall response to changes in the mechanical loading environment when compared with young mice due to diminished osteocyte signaling. In addition, we hypothesized that BCL-2 transgenic mice would also have a decreased

bone adaptation response to unloading and reloading compared to young wild-type mice similar to expected response of old mice. These findings would establish key differences in bone adaptation with age and osteocyte density that may have far-reaching implications for the treatment of elderly patients to maintain skeletal health during and after periods of disuse.

3.3 Methods

3.3.1 Animals

This study used a total of 93 C57Bl-6J male mice purchased from the Jackson Laboratory (Sacramento, CA) and 33 male BCL-2 transgenic mice bred at Lawrence Livermore National Laboratory (Livermore, CA) for a total of 126 animals. All mice in this study belonged to one of three experimental groups: Young WT mice (n=47) were 3-month-old C57Bl-6J mice, Old WT mice (n=46) were 18-month-old C57Bl-6J mice and Young BCL-2 Tg mice (n=34) were 3-month-old BCL-2 transgenic mice. In this study, we exclusively used male mice, as we wanted to evaluate trabecular bone changes in the distal femoral metaphysis, and male mice retain considerably more trabecular bone in their hindlimbs as they age compared to female mice⁷⁹. Mice were cared for in accordance with the guidelines set by the National Institutes of Health (NIH) on the care and use of laboratory animals. All procedures were approved by the Institutional Animal Care and Use Committee at UC Davis.

3.3.2 *Experimental groups and study design*

Mice were allowed to acclimate for 1-2 weeks in the vivarium prior to the start of the study. A subgroup of mice from each experimental group was euthanized at day 0 to establish baseline bone properties. All remaining mice underwent a period of tail suspension for up to 14 days as described below. One subgroup of mice from each experimental group was sacrificed after 2 days of tail suspension while remaining mice underwent 14 days of tail suspension. Another subgroup of mice was euthanized immediately after the unloading period without resuming normal cage activity. Remaining mice were allowed to resume normal cage activity (reloading) for either 2 or 14 days after the unloading period. Subgroups of Young WT and Old WT mice included 8-10 mice per time point. Subgroups of Young BCL-2 Tg mice included 6-8 mice per time point due to limited availability of animals. Experimental groups, terminal time points and group sizes are presented in Table 3.1.

At each terminal time point, mice were euthanized by exsanguination via cardiac puncture under anesthesia followed by cervical dislocation. Whole blood was collected during cardiac puncture for use in serum ELISA analysis described below and hindlimb bones were collected and stored in the methods described below for micro-computed tomography analysis or histology.

Table 3.1: Experimental groups, terminal time points for subgroups, and subgroup sizes

Experimental Group	Baseline (Day 0)	2 days of unloading (Day 2)	14 days of unloading (Day 14)	2 days of reloading (Day 16)	14 days of reloading (Day 28)
Young WT (3 months old)	n=9	n=10	n=8	n=10	n=10
Old WT (18 months old)	n=8	n=10	n=10	n=10	n=8
Young BCL-2 Tg (3 months old)	n=6	n=8	n=7	n=6	n=7

3.3.3 Hindlimb unloading via tail suspension

Mice were subjected to hindlimb unloading via tail suspension as first described by Morey-Holten⁴⁹. Mice were anesthetized through inhalation of 2.5% isoflurane. While anesthetized, the tail was sterilized with an alcohol wipe and a thin strip of skin-safe medical tape was wrapped around the base of the tail to minimize irritation. A U-shaped piece of wire was threaded through a swivel on an acrylic loop and was then attached to the wrapped base of the tail via cyanoacrylate. Once the wire hook was securely attached to the length of the tail, the hook and tail were wrapped with one thicker piece of skin-safe medical tape to reduce skin irritation and prevent mice from biting at the tail fixture. Mice were individually housed in custom-made cages with a rod across the top of the cage. The acrylic loop at the top of the hook assembly was placed on the rod at the top of the cage. This assembly allowed the mice to move around their cage and access food and water through their front limbs, but their hind limbs were unable to touch the floor of the cage (approximately 30-degree head-down angle).

3.3.4 Histology: TUNEL staining

Histology was used to qualify differences in osteocyte density and osteocyte apoptosis between the baseline mice of each experimental group (Young WT, Old WT and Young BCL2). Following euthanasia, right tibias were fixed in a 4% paraformaldehyde (PFA) solution for 5-7 days and then stored in 70% ethanol until decalcification. Tibias were decalcified with 0.5 M Ethylenediaminetetraacetic acid (EDTA) until decalcified as determined via Xray. Decalcified tibias (n=2 per subgroup, n=6 total) were processed for paraffin embedding and 6µm longitudinal sections were cut of the mid diaphysis to proximal end of the tibia. Sections were stained for Terminal deoxynucleotidyl transferase dUTP nick end labeling (TUNEL) using the Apoptag[®] system (Millipore Sigma, Temecula, CA). For each stained section, three areas of cortical bone were imaged at 20x magnification and analyzed for live and apoptotic osteocytes. Live osteocytes were stained blue while TUNEL positive apoptotic osteocytes were stained brown. Sections were analyzed for relative differences in osteocyte number, osteocyte apoptosis, and empty lacunae normalized to the surface area of the section analyzed.

3.3.5 Micro-computed tomography analysis of trabecular and cortical bone

Following euthanasia, left femurs were collected and preserved in 70% ethanol, then scanned via micro-computed tomography (SCANCo µCT 35, Brüttsellen, Switzerland) at X-ray tube potential 55 kVp, intensity 114 mA, integration time 900 ms, 6 µm isotropic nominal voxel size. Trabecular bone analysis was performed at the distal

metaphysis and distal epiphysis of the femur. Cortical bone analysis was performed at the mid diaphysis.

The epiphyseal region of interest began immediately proximal to the distal subchondral bone plate and included all trabecular bone between the subchondral bone plate and the distal growth plate. Because this section was fully enclosed by the growth plate, the size of region of interest for the epiphysis varied from sample to sample in the range of 70-110 slices or 0.42-0.66 mm in length. The metaphysis was defined as the trabecular bone within 200 slices (1.2mm) of the region immediately proximal to the distal growth plate. Trabecular bone parameters were calculated in both regions with the manufacturer's 3D analysis software and included: trabecular bone volume fraction (BV/TV), trabecular number (Tb.N), trabecular thickness (Tb.Th), and trabecular separation (Tb.Sp).

The region of interest for the cortical bone analysis was the mid diaphysis, defined as a 200 slice (1.2 mm) region centered on 50% of the femur's total length. Bone area (B.Ar), total cross-sectional area (T.Ar), bone area fraction (B.Ar/T.Ar), cortical thickness (Ct.Th), and other parameters were calculated using the manufacturer's 3D analysis software. Additional parameters needed to calculate material properties from three-point bending mechanical testing data were obtained from μ CT analysis, including the minimum moment of inertia (I_{min}) and the distance to the neutral axis (c).

3.3.6 *Three-point bending mechanical testing*

After μ CT scanning, left femurs were mechanically tested in three-point bending to determine structural and material properties. Prior to testing, femurs were rehydrated by submerging them in a solution of phosphate buffered saline for at least 10 minutes. Rehydrated femurs were then loaded into the mechanical testing machine (ELF 3200, TA Instruments, New Castle, DE) in a three-point bending setup such that the midpoint of the bone was directly beneath the top loading platen. The two lower platens were separated by 8 mm. To prevent motion or rotation of the bone during the test, the top actuator was lowered onto the sample to a preload of no more than 5N. Samples were tested with the posterior aspect of the bone loaded in tension. Femurs were loaded to failure by a single monotonic load at a rate of 0.01 mm/sec. Force and displacement data were recorded at 50 Hz. Using the output force-displacement data, the linear region was isolated, and the yield point was identified as the point at which the force-displacement curve became non-linear. Stiffness of the linear region (K), yield force (F_Y), and ultimate force (F_{ult}) were determined from the force-displacement curve. Minimum moment of inertia (I_{min}) and the distance to the neutral axis (c) were used to calculate elastic modulus (E), yield stress, and ultimate stress using beam theory equations¹³².

3.3.7 *Serum cytokine analysis*

Blood samples were collected at the time of euthanasia from cardiac puncture. Blood was stored in uncoated Eppendorf tubes and allowed to clot at room temperature for 1 hour. The blood was then spun at 1000g for 10 minutes at 4°C and the serum was

pipetted off. Serum samples were stored at -80°C until analyzed. Enzyme-linked immunosorbent assay (ELISA) was used to measure circulating levels of three inflammatory cytokines, Interleukin 6 (IL-6), Interleukin 1 beta (IL-1 β) and tumor necrosis factor alpha (TNF α), in the isolated serum using a kit (Meso Scale Discovery, Rockville, MD) according to the manufacturer's instructions.

3.3.8 Statistical analysis

Statistical analysis on μCT , mechanical testing and ELISA results was performed via 2-way ANOVA stratified by experimental group and time point with statistical significance defined as $p < 0.05$. Main effect differences between experimental groups were obtained through the ANOVA. Old WT and Young BCL-2 Tg mice differ both in age and genotype, thus no direct statistical comparisons were made between these two groups. Instead, both of those experimental groups were compared only to Young WT mice.

To determine differences between subgroups (time points) within each experimental group, post-hoc planned contrasts were performed. To adjust for the multiple comparisons from planned contrasts, the cutoff p-value for statistical significance was adjusted with a Bonferroni correction. The p-value (originally set at $p < 0.05$) was divided by the total number of contrasts which was 30. This is because 10 contrasts were performed in each mouse experimental group to obtain all comparisons within a group

and there were three experimental group. Thus, statistical significance in each planned contrast was defined as $p < 0.00167$.

3.4 Results

3.4.1 Histology: TUNEL staining

Histological assessment of baseline samples showed that Old WT mice (Fig. 3.1b) had lower osteocyte density and more extensive osteocyte apoptosis than Young WT mice (Fig. 3.1a). Lacunar density in Young BCL-2 Tg mice (Fig. 3.1c) was greater than that of either Young or Old WT mice. As can be seen in the images, osteocyte density is noticeably lower in the Old WT sample than the other two. In addition, there were empty lacunae present in samples from both Old WT mice and Young BCL-2 Tg mice, but no empty lacunae were visible in the TUNEL stained sections from Young WT mice.

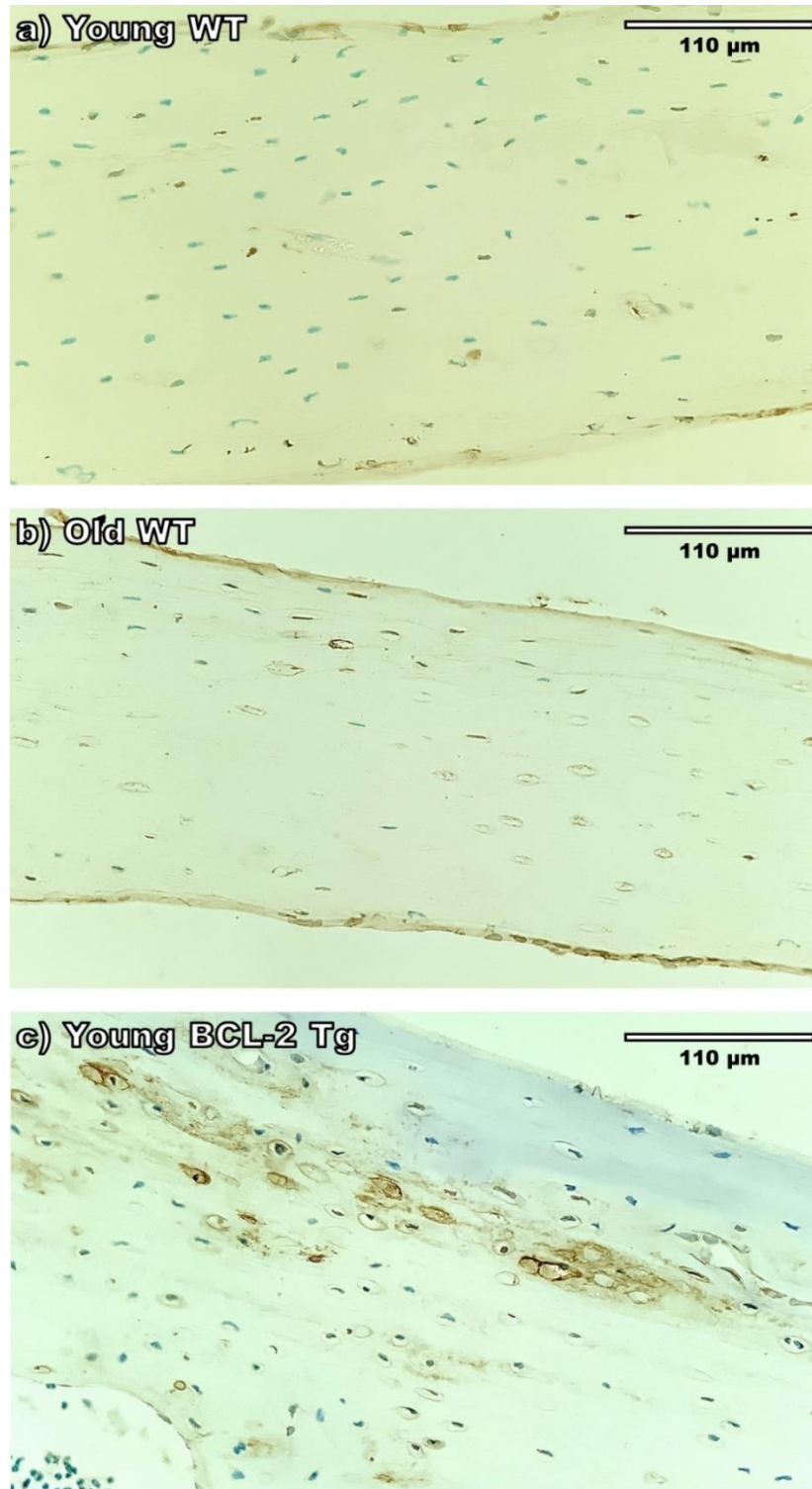


Figure 3.1: TUNEL Staining of cortical bone in representative baseline samples of (a) Young WT, (b) Old WT and (c) Young BCL-2 Tg mice. In the images, live osteocytes are stained blue, apoptotic osteocyte are stained brown and the outline of empty lacunae are also present in the Old WT and Young BCL2-Tg samples

The average number of live osteocytes, dead osteocyte and empty lacunae were recorded for each section and these averages were normalized across the area of bone analyzed in the sections (Fig. 3.2). Though it is a limited sample size representing two mice per experimental group, the total number of live or dead osteocytes in Old WT mice was lower than either Young WT or Young BCL2 Tg mice. Young WT and Young BCL-2 Tg samples had a similar average number of live or dead osteocytes. However, more apoptotic osteocytes were present in Young BCL-2 Tg mice than in Young WT mice, so the percentage of live osteocytes was decreased.

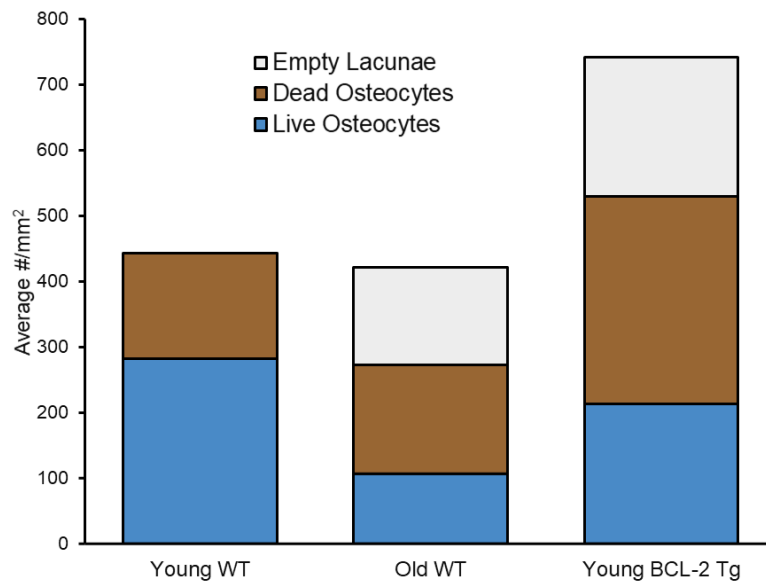


Figure 3.2: Normalized number of live and dead osteocytes and empty lacunae. The average number of live and dead osteocyte and empty lacunae were normalized to the bone area of the section analyzed for Young WT, Old WT and Young BCL-2 Tg baseline samples.

3.4.2 Micro-Computed Tomography Analysis: Young WT Mice

Young WT mice exhibited a large magnitude of bone loss during unloading at both trabecular sites, and a smaller magnitude of cortical bone loss. Trabecular bone loss was

largely recovered during reloading. However, cortical bone loss persisted during the reloading period. Full data from μ CT analyses of the three bone sites are presented in Table 3.2.

Table 3.2: Young WT μ CT analysis data. Data are presented as mean \pm standard deviation. A main effect difference between Young WT and Old WT in a parameter is denoted by (#) while a main effect difference between Young WT and Young BCL-2 Tg in a parameter is denoted by (^). Letters underneath the data indicate differences between subgroups of Young WT mice, subgroups that do not share a letter are statistically different.

	Baseline	<i>Experimental time points: Young WT Mice</i>			
		2d unloaded	14d unloaded	2d reloaded	14d reloaded
<i>Epiphysis</i>					
BV/TV # ^	0.3254 \pm 0.0297 A	0.2984 \pm 0.0359 AB	0.2376 \pm 0.0296 C	0.2167 \pm 0.0145 C	0.2877 \pm 0.0128 B
Tb.N # (1/mm)	6.6311 \pm 0.6709 A	6.7827 \pm 0.3317 A	6.2769 \pm 0.2902 AB	6.0624 \pm 0.2688 B	6.4605 \pm 0.1751 AB
Tb.Th # ^ (mm)	0.0526 \pm 0.0024 A	0.0471 \pm 0.0047 B	0.0406 \pm 0.0033 C	0.0373 \pm 0.0019 C	0.0480 \pm 0.0021 AB
Tb.Sp # ^ (mm)	0.1536 \pm 0.0177 A	0.1477 \pm 0.0080 A	0.1591 \pm 0.0069 A	0.1626 \pm 0.0074 A	0.1545 \pm 0.0048 A
<i>Metaphysis</i>					
BV/TV # ^	0.1966 \pm 0.0292 A	0.1624 \pm 0.0414 AB	0.1388 \pm 0.0106 BC	0.1130 \pm 0.0146 C	0.1270 \pm 0.0122 BC
Tb.N # ^ (1/mm)	5.894 \pm 0.5836 A	5.865 \pm 0.2916 A	5.571 \pm 0.1600 AB	5.388 \pm 0.2123 AB	5.130 \pm 0.1548 B
Tb.Th # ^ (mm)	0.0464 \pm 0.0042 A	0.0393 \pm 0.0071 B	0.0341 \pm 0.0029 B	0.03063 \pm 0.0019 C	0.0374 \pm 0.0026 BC
Tb.Sp # ^ (mm)	0.1652 \pm 0.0198 B	0.1665 \pm 0.0075 AB	0.1740 \pm 0.0053 AB	0.1805 \pm 0.0078 AB	0.1882 \pm 0.0059 A
<i>Diaphysis</i>					
Ct.Th ^ (mm)	0.1908 \pm 0.0034 A	0.1784 \pm 0.0151 AB	0.1791 \pm 0.0080 AB	0.1745 \pm 0.0062 B	0.1698 \pm 0.0109 B
B.Ar # ^ (mm²)	0.9509 \pm 0.0743 A	0.9049 \pm 0.0848 A	0.9414 \pm 0.0548 A	0.8789 \pm 0.0649 A	0.8992 \pm 0.0550 A
T.Ar # ^ (mm²)	1.987 \pm 0.1926 A	2.100 \pm 0.0976 A	2.197 \pm 0.1592 A	2.027 \pm 0.1324 A	2.232 \pm 0.1183 A
B.Ar./T.Ar # ^	0.4801 \pm 0.0178 A	0.4307 \pm 0.0324 B	0.4295 \pm 0.0200 B	0.4335 \pm 0.0136 B	0.4041 \pm 0.0284 B
I_{min} (mm⁴)	0.1564 \pm 0.0280 A	0.1622 \pm 0.0188 A	0.1754 \pm 0.0219 A	0.1505 \pm 0.0190 A	0.1746 \pm 0.0225 A
c # (mm)	0.6656 \pm 0.0368 B	0.6976 \pm 0.0228 AB	0.7247 \pm 0.0314 A	0.6972 \pm 0.0355 AB	0.7255 \pm 0.0301 A

During unloading, Young WT mice exhibited large decreases in some epiphyseal trabecular bone parameters. BV/TV was significantly lower (-27.0%) after 14 days of unloading compared to baseline values ($p < 0.0001$) (Fig 3.3a and Fig 3.4a). Meanwhile, Tb.Th in the epiphysis was 10.4% lower at 2 days of unloading compared to baseline ($p = 0.0011$) and was another 13.7% lower at 14 days of unloading compared to 2 days of unloading ($p = 0.0007$) (Fig 3.3b and Fig 3.4b).

During reloading, epiphyseal trabecular bone parameters in Young WT mice did not recover after 2 days of reloading but largely returned to baseline values after 14 days of reloading. After 2 days of reloading, BV/TV and Tb.Th remained lowered (-33.4% and -8.5% respectively) than baseline values ($p < 0.0001$ and $p = 0.0010$ respectively). After 14 days of reloading, Tb.Th returned to baseline values, but BV/TV remained lowered (-11.6%, $p = 0.0013$). Though there was a significant decrease in Tb.N during early reloading, Tb.N returned to baseline values after 14 days of reloading.

At the metaphysis, bone loss was observed during unloading in some parameters but not in others. Bone loss that occurred in unloading continued in early reloading and most parameters did not recover during reloading. After 14 days of unloading, BV/TV and Tb.Th were significantly lower (-29.4% and -26.6% respectively) than baseline ($p = 0.0005$ and $p < 0.0001$ respectively) (Fig 3.3c-d and Fig 3.4c-d). Metaphyseal BV/TV and Tb.Th values remained lower than baseline during reloading as well.

Most cortical bone parameters did not change over the unloading period, however there was some bone loss observed in early reloading. While Ct.Th was not significantly different after 14 days of unloading in Young WT mice (Fig 3.3e and Fig 3.4e), the cortical bone area fraction, B.Ar/T.Ar, was significantly lower than baseline (-10.3%) in Young WT mice after 2 days of unloading ($p = 0.0009$). After 14 days of reloading, Ct.Th in Young WT mice was significantly lower (-11.0%) than the baseline value ($p = 0.0006$) and B.Ar/T.Ar remained significantly lower than baseline through the reloading period.

3.4.3 Micro-computed Tomography Analysis: Old WT Mice

Old WT mice exhibited bone loss at both trabecular bone sites during unloading that continued during early reloading for some trabecular bone parameters (Table 3.3). Some trabecular bone parameters began to recover by the end of reloading, while others did not. Old WT mice also experienced bone loss in the cortical bone during unloading which was not recovered during reloading. Main effect differences of mouse experimental group were present in all trabecular bone parameters at both sites between Old WT and Young WT mice, with Old WT mice having overall lower trabecular BV/TV, Tb.Th. and Tb.N and higher Tb.Sp. In the cortical bone, Old WT mice had overall greater B.Ar, and T.Ar.

Table 3.3: Old WT μ CT analysis data. Data are presented as mean \pm standard deviation. Significant main effect differences between Young WT and Old WT mice in a parameter are denoted by (#) symbol. Letters underneath the data indicate differences within subgroups of Old WT mice, subgroups that do not share a letter are statistically different.

		<i>Experimental time points: Old WT Mice</i>				
		<i>Baseline</i>	<i>2d unloaded</i>	<i>14d unloaded</i>	<i>2d reloaded</i>	<i>14d reloaded</i>
<i>Epiphysis</i>						
BV/TV	#	0.3020 \pm 0.0171 N	0.2637 \pm 0.0314 NO	0.1957 \pm 0.0206 OP	0.1782 \pm 0.0145 P	0.2298 \pm 0.0105 O
Tb.N	# (1/mm)	5.609 \pm 0.2877 N	5.302 \pm 0.3663 NO	4.862 \pm 0.2766 O	4.932 \pm 0.0962 O	5.032 \pm 0.2725 NO
Tb.Th	# (mm)	0.0606 \pm 0.0036 N	0.0548 \pm 0.0043 O	0.0445 \pm 0.0039 P	0.0386 \pm 0.0022 Q	0.0487 \pm 0.0021 P
Tb.Sp	# (mm)	0.1818 \pm 0.0080 O	0.1913 \pm 0.0142 NO	0.2039 \pm 0.0162 N	0.2027 \pm 0.0054 N	0.1973 \pm 0.0095 NO
<i>Metaphysis</i>						
BV/TV	#	0.0816 \pm 0.0166 N	0.0850 \pm 0.0159 N	0.0411 \pm 0.0103 O	0.0437 \pm 0.0098 O	0.0512 \pm 0.0165 NO
Tb.N	# (1/mm)	2.958 \pm 0.2330 N	2.772 \pm 0.2508 N	2.549 \pm 0.2125 N	2.692 \pm 0.2214 N	2.766 \pm 0.1534 N
Tb.Th	# (mm)	0.0545 \pm 0.0043 N	0.0550 \pm 0.0072 N	0.0351 \pm 0.0039 O	0.0332 \pm 0.0040 O	0.0376 \pm 0.0071 O
Tb.Sp	# (mm)	0.3351 \pm 0.0259 O	0.3617 \pm 0.0369 NO	0.3900 \pm 0.0346 N	0.3679 \pm 0.0318 NO	0.3566 \pm 0.0207 NO
<i>Diaphysis</i>						
Ct.Th	# (mm)	0.1955 \pm 0.0114 N	0.1894 \pm 0.0058 N	0.1731 \pm 0.0112 O	0.1650 \pm 0.0103 O	0.1616 \pm 0.0097 O
B.Ar	# (mm ²)	0.9509 \pm 0.0743 N	0.9049 \pm 0.0848 N	0.9414 \pm 0.0548 NO	0.8789 \pm 0.0649 O	0.8992 \pm 0.0550 O
T.Ar	# (mm ²)	2.661 \pm 0.1671 N	2.674 \pm 0.1254 N	2.741 \pm 0.1603 N	2.607 \pm 0.1267 N	2.678 \pm 0.1864 N
B.Ar./T.Ar	#	0.4134 \pm 0.0197 N	0.4017 \pm 0.0108 N	0.3648 \pm 0.0261 O	0.3567 \pm 0.0188 O	0.3551 \pm 0.0116 O
I_{min}	# (mm ⁴)	0.2557 \pm 0.0320 N	0.2551 \pm 0.0188 N	0.2467 \pm 0.0258 N	0.2176 \pm 0.0283 N	0.2229 \pm 0.0247 N
c	# (mm)	0.8050 \pm 0.0259 N	0.7933 \pm 0.0289 N	0.8349 \pm 0.0324 N	0.8023 \pm 0.0363 N	0.8155 \pm 0.0207 N

After 14 days of unloading, bone loss was observed in all epiphyseal trabecular bone parameters in the femurs of Old WT mice. Both BV/TV and Tb.N were significantly lower (-35.2% and -13.3% respectively) after 14 days of unloading compared to baseline ($p < 0.0001$ and $p < 0.0001$) (Fig 3.3a). In addition, Tb.Sp was 12.1% higher at 14 days

of unloading compared to baseline ($p = 0.0002$). Tb.Th in Old WT mice was 9.6% lower than baseline after only 2 days of unloading ($p = 0.0005$) and was another 18.7% lower at 14 days of unloading compared to 2 days of unloading ($p < 0.0001$) (Fig 3.3b).

Following reloading, epiphyseal trabecular bone parameters mice significantly recovered towards baseline values but remained significantly lower than baseline. After 14 days of reloading, BV/TV remained 23.9% lower than baseline BV/TV ($p < 0.0001$). Meanwhile, during early reloading, Tb.Th further decreased (-13.4%) after 2 days of reloading than the 14 days of unloading time point ($p = 0.0005$). By 14 days of reloading, Tb.Th remained 19.6% lower than baseline values ($p < 0.0001$).

In the metaphysis, though there was much less trabecular bone in this region, there was some trabecular bone loss during unloading. In Old WT mice, Tb.Th was significantly lower (-35.6%) at 14 days of unloading compared to baseline ($p < 0.0001$) and remained lower than baseline for the full reloading period (Fig 3.3d). In addition, BV/TV in Old WT mice was 46.4% lower at 14 days of unloading compared to baseline ($p < 0.0001$) (Fig 3.3c).

Finally, in the cortical bone, bone loss occurred during unloading and early reloading. Old WT mice had significantly lower Ct.Th (-11.5%) at 14 days of unloading compared to baseline values ($p = 0.0005$) (Fig. 3.3e). After 2 days of reloading, B.Ar was significantly lower (-15.3%) than baseline values at 2 days of reloading ($p < 0.0001$) (Fig

3.3f). Meanwhile, Ct.Th in Old WT mice remained low and ended 17.3% lower than baseline after 14 days of unloading ($p < 0.0001$).

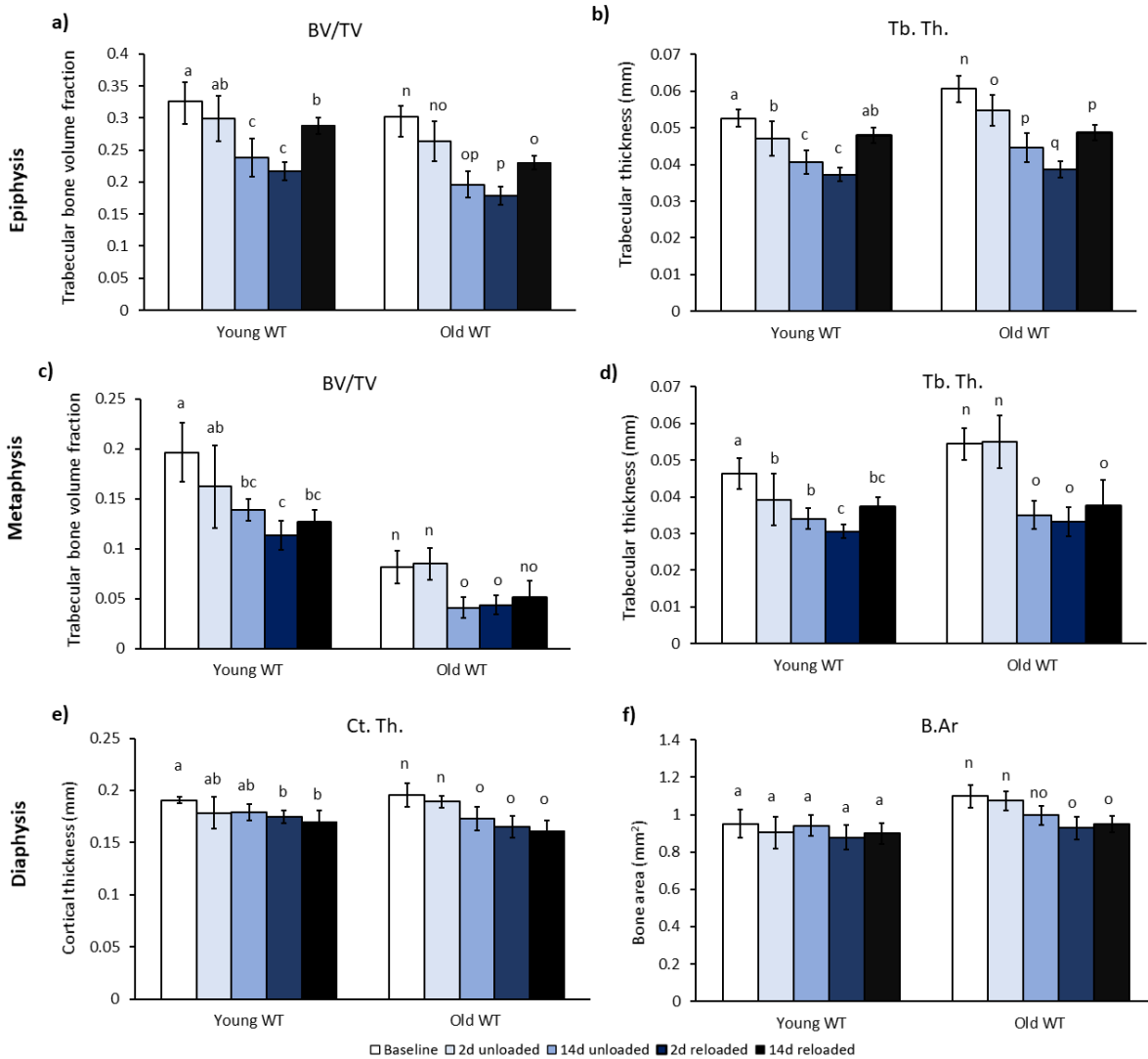


Figure 3.3: Comparison of Young WT and Old WT μ CT results. Epiphyseal BV/TV (3.2a) and Tb.Th. (3.2b), Metaphyseal BV/TV (3.2c) and Tb.Th. (3.2d) and mid-diaphysis Ct.Th and B.Ar results for Young WT and Old WT mice after 14 days of unloading followed by 14 days of reloading. Data are presented as means with standard deviations as error bars. Letters indicate a significant difference between subgroups within a mouse experimental group, subgroups that do not share a letter are significantly different.

3.4.4 Micro-Computed Tomography Analysis: Young BCL-2 Tg Mice

During unloading, the bones of Young BCL-2 Tg mice exhibited some trabecular bone loss in both the epiphysis and the metaphysis. However, unlike Young WT mice, there was no recovery observed in trabecular bone properties during reloading. In addition, cortical bone did not respond to either unloading or reloading. Young BCL-2 Tg mice exhibited generally higher trabecular bone properties, such as BV/TV and Tb.Th., than Young WT mice. Young BCL-2 Tg mice also had greater Ct.Th, B.Ar, T.Ar and B.Ar./T.Ar.

Table 3.3: Young BCL-2 Tg μ CT analysis data. Data are presented as mean \pm standard deviation. Significant main effect differences between Young WT and Young BCL-2 Tg mice in a parameter are denoted by (^) symbol. Letters underneath the data indicate differences within subgroups of Young BCL-2 Tg mice, subgroups that do not share a letter are statistically different.

	Baseline	Experimental time points: Young BCL-2 Tg Mice			
		2d unloaded	14d unloaded	2d reloaded	14d reloaded
<i>Epiphysis</i>					
BV/TV ^	0.3544 \pm 0.0165 X	0.3320 \pm 0.0343 X	0.2538 \pm 0.0301 Y	0.2440 \pm 0.0184 Y	0.2752 \pm 0.0158 Y
Tb.N (1/mm)	6.876 \pm 0.3579 X	6.817 \pm 0.5115 X	5.860 \pm 0.3210 Y	6.082 \pm 0.2285 Y	5.842 \pm 0.2031 Y
Tb.Th ^ (mm)	0.0563 \pm 0.0015 X	0.0535 \pm 0.0029 X	0.0455 \pm 0.0039 Y	0.0432 \pm 0.0034 Y	0.0487 \pm 0.0013 XY
Tb.Sp ^ (mm)	0.1517 \pm 0.0085 Y	0.1524 \pm 0.0127 Y	0.1771 \pm 0.0093 X	0.1679 \pm 0.0055 XY	0.1734 \pm 0.0049 X
<i>Metaphysis</i>					
BV/TV ^	0.2738 \pm 0.0309 X	0.2383 \pm 0.0578 X	0.2395 \pm 0.0294 X	0.2100 \pm 0.0098 XY	0.1527 \pm 0.0403 Y
Tb.N ^ (1/mm)	6.969 \pm 0.3063 X	6.533 \pm 0.6070 XY	6.391 \pm 0.2893 XY	6.056 \pm 0.6796 Y	5.135 \pm 0.4410 Z
Tb.Th ^ (mm)	0.0488 \pm 0.0030 X	0.0464 \pm 0.0052 X	0.0450 \pm 0.0027 XY	0.0415 \pm 0.0039 XY	0.0380 \pm 0.0035 Y
Tb.Sp ^ (mm)	0.1418 \pm 0.0066 Y	0.1520 \pm 0.0161 Y	0.1544 \pm 0.0083 XY	0.1627 \pm 0.0188 XY	0.1917 \pm 0.0203 X

<i>Diaphysis</i>					
Ct.Th ^ (mm)	0.1908 ± 0.0034 X	0.1784 ± 0.0151 X	0.1791 ± 0.0080 X	0.1745 ± 0.0062 X	0.1698 ± 0.0109 X
B.Ar ^ (mm ²)	0.9509 ± 0.0743 X	0.9049 ± 0.0848 X	0.9414 ± 0.0548 X	0.8789 ± 0.0649 X	0.8992 ± 0.0550 X
T.Ar ^ (mm ²)	1.987 ± 0.1926 X	2.100 ± 0.0976 X	2.197 ± 0.1592 X	2.027 ± 0.1324 X	2.232 ± 0.1183 X
B.Ar./T.Ar ^	0.4801 ± 0.0178 X	0.4307 ± 0.0324 X	0.4295 ± 0.0200 X	0.4335 ± 0.0136 X	0.4041 ± 0.0284 X
I_{min} (mm ⁴)	0.1564 ± 0.0280 X	0.1622 ± 0.0188 X	0.1754 ± 0.0219 X	0.1505 ± 0.0190 X	0.1746 ± 0.0225 X
c (mm)	0.6656 ± 0.0368 Y	0.6976 ± 0.0228 XY	0.7247 ± 0.0314 XY	0.6972 ± 0.0355 X	0.7255 ± 0.0301 Y

In the epiphysis, we observed trabecular bone loss following unloading and this loss did not recover during reloading. BV/TV was lower (-28.3%) compared to baseline after 14 days of unloading ($p < 0.0001$). In addition, Tb.N and Tb.Th (-14.8% and -19.1% respectively) were lower after 14 days of unloading compared to baseline ($p = 0.0007$ and $p < 0.0001$ respectively). Tb.Sp was higher (+16.7%) after 14 days of unloading compared to baseline ($p = 0.0008$). During reloading no trabecular bone parameters in the epiphysis exhibited any recovery.

Meanwhile, in the metaphysis, no trabecular bone parameters were different from baseline after unloading. However, bone loss was observed in during reloading in some parameters. At the end of the study, after 14 days of unloading, both BV/TV and Tb.Th were significantly lower (-44.2% and -21.6% respectively) than baseline values ($p < 0.0001$ and $p = 0.0005$ respectively) (Fig 3.4c-d).

Throughout the full unloading and reloading period, we observed no changes in cortical bone properties in the Young BCL-2 Tg mice (Fig 3.4e-f).

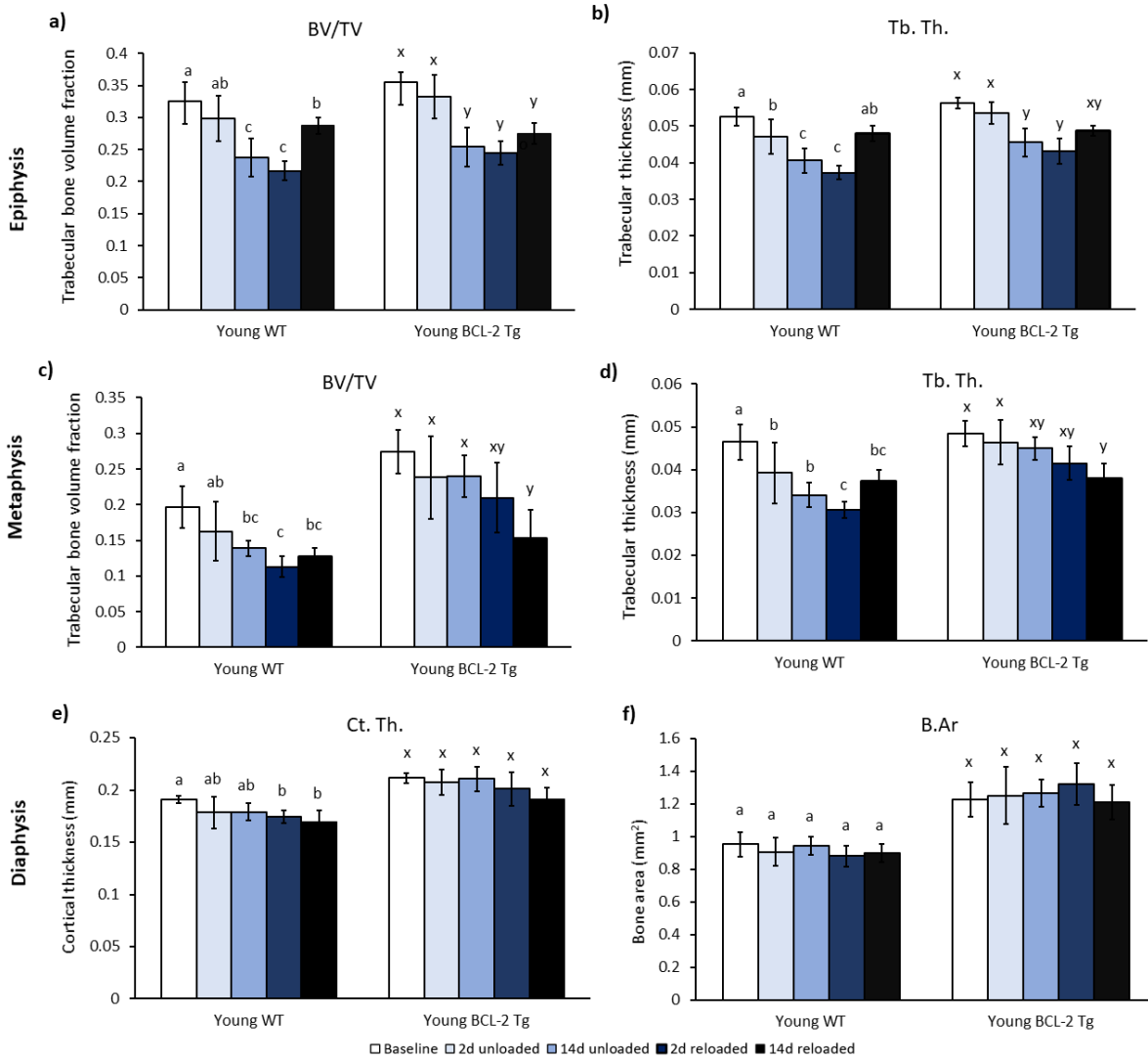


Figure 3.4: Comparison of Young WT and Young BCL-2 Tg μ CT results. Epiphyseal BV/TV (3.2a) and Tb.Th. (3.2b), Metaphyseal BV/TV (3.2c) and Tb.Th. (3.2d) and mid-diaphysis Ct.Th (3.2e) and B.Ar (3.2f) results for Young WT and Young BCL-2 Tg mice after 14 days of unloading followed by 14 days of reloading. Data are presented as means with standard deviations as error bars. Letters indicate a significant difference between subgroups within a mouse experimental group, subgroups that do not share a letter are significantly different.

3.4.5 Mechanical Testing

Three-point bending results largely mirrored the results from the cortical bone structure analysis in each experimental group (Table 3.5). We observed significant decreases in mechanical properties following unloading in the bones of Old WT and Young WT mice. In the Young BCL-2 Tg mice in which we observed no changes in cortical bone properties in response to any change in loading environment, we observed no changes in bone mechanical properties in response to changes in loading environment.

We also observed main effect differences between experimental groups. All the mechanical properties of bones of Old WT mice were lower than those of the Young WT mice. Meanwhile, the mechanical properties bones of the Young BCL-2 Tg mice also had main effect differences from the bones of the Young WT mice. Young BCL-2 femurs had significantly higher stiffness, yield and ultimate force, and yield and ultimate stress.

Table 3.5: Three-point bending mechanical testing data. Data are presented as mean \pm standard deviation. A main effect difference between Young WT and Old WT in a parameter is denoted by (#) while a main effect difference between Young WT and Young BCL-2 Tg in a parameter is denoted by (^). Letters underneath the data indicated differences between subgroups within a single experimental group (Young WT, Old WT and Young BCL-2 Tg), subgroups that do not share a letter are statistically different.

	Baseline	2d unloaded	Experimental time points		
			14d unloaded	2d reloaded	14d reloaded
<i>Young WT</i>					
K # ^ (N/mm)	132.4 \pm 13.50 A	105.9 \pm 25.82 A	123.8 \pm 8.131 A	108.8 \pm 9.536 A	108.9 \pm 14.47 A
F_Y # ^ (N)	14.59 \pm 1.825 A	11.39 \pm 3.142 A	12.59 \pm 1.303 A	12.26 \pm 2.154 A	11.62 \pm 3.242 A
F_{ult} # ^ (N)	17.68 \pm 1.763 A	15.62 \pm 2.921 A	17.67 \pm 0.649 A	16.61 \pm 1.747 A	15.56 \pm 2.282 A
E # (GPa)	9.388 \pm 2.389 A	6.997 \pm 1.236 B	7.646 \pm 1.076 AB	7.722 \pm 0.7390 AB	6.765 \pm 1.237 B
σ_Y # ^ (MPa)	129.3 \pm 37.22 A	98.31 \pm 20.60 A	105.4 \pm 15.71 A	114.2 \pm 20.43 A	97.48 \pm 28.07 A
σ_{ult} # ^ (MPa)	155.2 \pm 33.12 A	135.5 \pm 16.49 A	147.3 \pm 10.25 A	154.3 \pm 13.99 A	130.7 \pm 22.18 A
<i>Old WT</i>					
K # (N/mm)	129.0 \pm 32.85 N	121.7 \pm 16.86 N	86.57 \pm 23.52 O	69.95 \pm 14.21 O	62.75 \pm 19.21 O
F_Y # (N)	11.28 \pm 2.883 N	10.75 \pm 2.764 N	8.326 \pm 2.277 N	7.881 \pm 1.276 N	7.448 \pm 1.684 N
F_{ult} # (N)	17.33 \pm 3.038 N	15.52 \pm 1.326 NO	12.09 \pm 1.175 O	10.95 \pm 1.069 O	11.42 \pm 1.304 O
E # (GPa)	5.398 \pm 1.259 N	5.116 \pm 0.798 NO	3.786 \pm 1.080 NO	3.460 \pm 0.6800 NO	3.044 \pm 1.056 O
σ_Y # (MPa)	70.89 \pm 15.81 N	67.06 \pm 17.87 N	57.62 \pm 18.39 N	58.49 \pm 9.016 N	54.23 \pm 10.52 N
σ_{ult} # (MPa)	109.3 \pm 14.63 N	96.69 \pm 7.406 NO	82.40 \pm 9.377 O	81.34 \pm 8.169 O	84.27 \pm 11.66 O
<i>Young BCL-2 Tg</i>					
K ^ (N/mm)	166.9 \pm 32.78 X	176.5 \pm 33.90 X	167.4 \pm 23.26 X	170.0 \pm 27.62 X	161.0 \pm 21.25 X
F_Y ^ (N)	19.54 \pm 2.079 X	20.72 \pm 3.255 X	20.68 \pm 4.212 X	22.72 \pm 2.564 X	18.95 \pm 4.398 X
F_{ult} ^ (N)	26.13 \pm 3.474 X	25.80 \pm 4.510 X	27.28 \pm 4.230 X	27.51 \pm 3.325 X	24.04 \pm 4.081 X
E (GPa)	8.786 \pm 0.9070 X	8.411 \pm 0.7292 X	7.622 \pm 0.8030 X	6.954 \pm 1.034 X	8.341 \pm 0.7139 X
σ_Y ^ (MPa)	134.0 \pm 13.66 X	132.1 \pm 13.80 X	128.4 \pm 18.40 X	134.7 \pm 13.01 X	127.8 \pm 20.61 X
σ_{ult} ^ (MPa)	178.4 \pm 13.93 X	163.1 \pm 10.44 X	170.3 \pm 13.77 X	162.7 \pm 14.28 X	162.8 \pm 16.66 X

In Young WT mice, there were not many changes in mechanical properties in the femurs in response to unloading or reloading. The only difference was in the elastic modulus which was 25.4% lower after 2 days of unloading ($p < 0.0001$) (Fig 3.5b and 3.6b). The modulus would remain lower than baseline after 14 days of reloading.

The unloading period affected multiple mechanical properties in the femurs of Old WT mice. All mechanical properties that decreased during unloading would show no recovery during the reloading period. After 14 days of unloading, femurs from Old WT mice had a significantly lower stiffness (-32.8%) than baseline values ($p = 0.0038$), and ultimate force was significantly lower (-30.2%) than baseline ($p < 0.0001$) (Fig 3.5a and Fig 3.5c). During reloading, stiffness and ultimate force remained significantly lower than baseline for the duration of the study. After 14 days of reloading, the elastic modulus was significantly lower (-43.6%) than baseline ($p < 0.0005$) (Fig 3.5b).

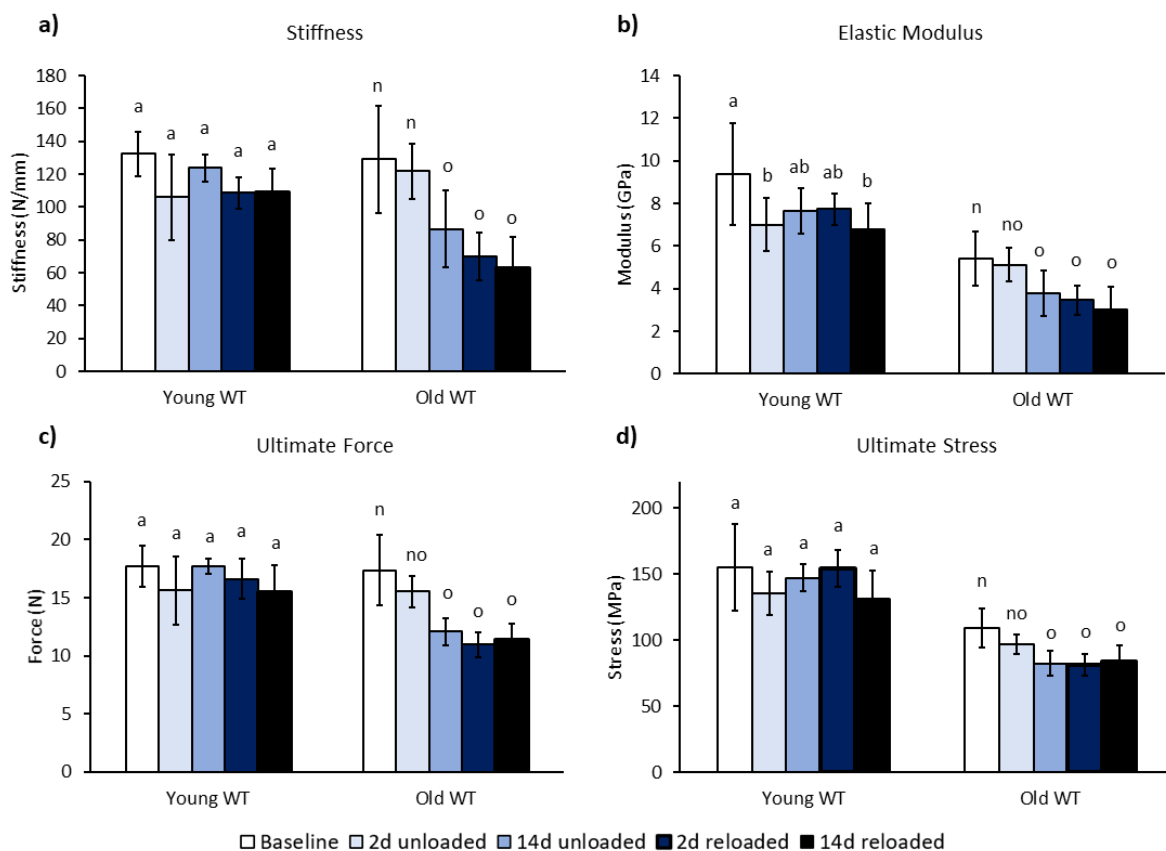


Figure 3.5: Comparison of Young WT and Old WT three-point bending results. Stiffness (3.4a), elastic modulus (3.4b), ultimate force. (3.4c), and ultimate stress (3.4d) results for Young WT and Old WT results after 14 days of unloading followed by 14 days of reloading. Data are presented as means with standard deviations as error bars. Letters indicate a significant difference between subgroups within a mouse experimental group, subgroups that do not share a letter are significantly different.

As previously described, there were no significant differences in the mechanical properties between subgroups of Young BCL-2 Tg mice (Fig 3.6a-d). The only statistically significant differences were the main effect differences between the two experimental groups of Young WT and Young BCL-2 Tg mice described above.

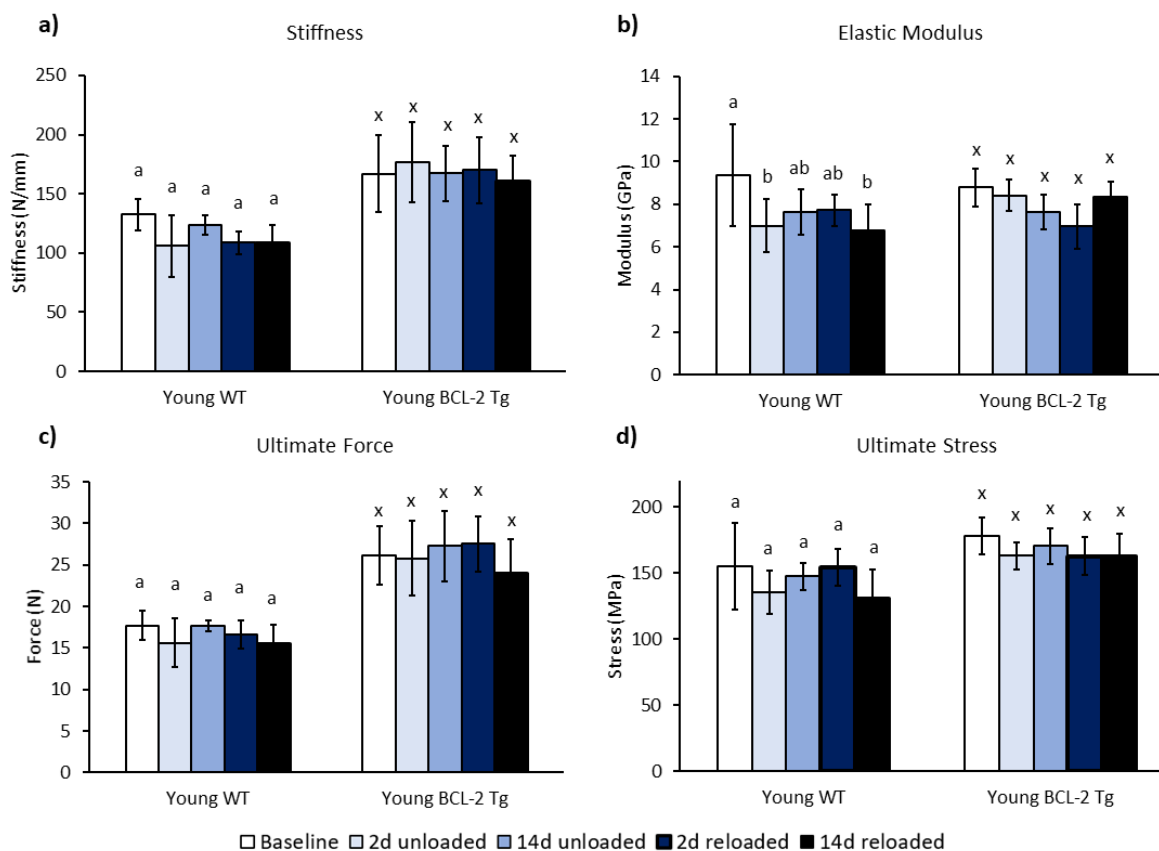


Figure 3.6: Comparison of Young WT and Young BCL-2 Tg three-point bending results. Stiffness (3.4a), elastic modulus (3.4b), ultimate force. (3.4c), and ultimate stress (3.4d) results for Young WT and Young BCL-2 Tg mice after 14 days of unloading followed by 14 days of reloading. Data are presented as means with standard deviations as error bars. Letters indicate a significant difference between subgroups within a mouse experimental group, subgroups that do not share a letter are significantly different.

3.4.6 Serum Cytokine Analysis

Serum cytokine measures had high variability within subgroups, and thus we observed significant main effects between experimental groups, but no differences due to unloading or reloading (Table 3.6). As a main effect, Young WT mice had higher IL-1 β than Old WT mice and lower TNF- α than Old WT mice ($p < 0.0001$ and $p < 0.0001$

respectively). In addition, Young WT mice had higher IL-1 β than Young BCL-2 Tg mice ($p < 0.0001$) (Fig 3.7).

Table 3.6 Serum cytokine ELISA data. Serum concentrations of IL-1B, TNF- α , and IL-6. Data are presented as mean \pm standard deviation. A main effect difference between Young WT and Old WT in a cytokine is denoted by (#) while a main effect difference between Young WT and Young BCL-2 Tg in a cytokine is denoted by (^). There were no statistically significant differences between subgroups within any of the three mouse experimental groups (Young WT, Old WT and Young BCL-2 Tg).

	Baseline	Experimental time points			
		2d unloaded	14d unloaded	2d reloaded	14d reloaded
<i>Young WT</i>					
IL-1 β # ^ (pg/ml)	1.234 \pm 0.5821	0.6720 \pm 0.4294	0.8900 \pm 0.4337	0.7324 \pm 0.4960	0.3556 \pm 0.2001
TNF α # (pg/ml)	8.642 \pm 2.823	5.585 \pm 0.6173	6.358 \pm 0.6929	6.087 \pm 1.931	5.047 \pm 0.6206
IL-6 (pg/ml)	65.87 \pm 63.98	19.70 \pm 14.61	96.54 \pm 138.5	16.90 \pm 12.79	2.821 \pm 1.043
<i>Old WT</i>					
IL-1 β # (pg/ml)	0.7926 \pm 0.5574	0.5817 \pm 0.3207	0.6587 \pm 0.3238	0.4232 \pm 0.2363	0.2940 \pm 0.0942
TNF α # (pg/ml)	12.89 \pm 4.534	8.533 \pm 2.485	9.755 \pm 3.095	8.568 \pm 1.933	13.64 \pm 16.56
IL-6 (pg/ml)	198.3 \pm 167.7	33.46 \pm 20.10	71.06 \pm 69.45	60.52 \pm 85.44	24.52 \pm 25.64
<i>Young BCL-2 Tg</i>					
IL-1 β ^ (pg/ml)	0.4819 \pm 0.2809	0.4113 \pm 0.2889	0.5066 \pm 0.1828	0.4688 \pm 0.2123	0.3112 \pm 0.1188
TNF α (pg/ml)	8.665 \pm 1.651	6.598 \pm 0.7913	6.997 \pm 1.552	7.289 \pm 1.131	6.627 \pm 0.9809
IL-6 (pg/ml)	101.4 \pm 110.6	22.68 \pm 15.24	121.7 \pm 205.5	47.96 \pm 34.68	5.550 \pm 2.549

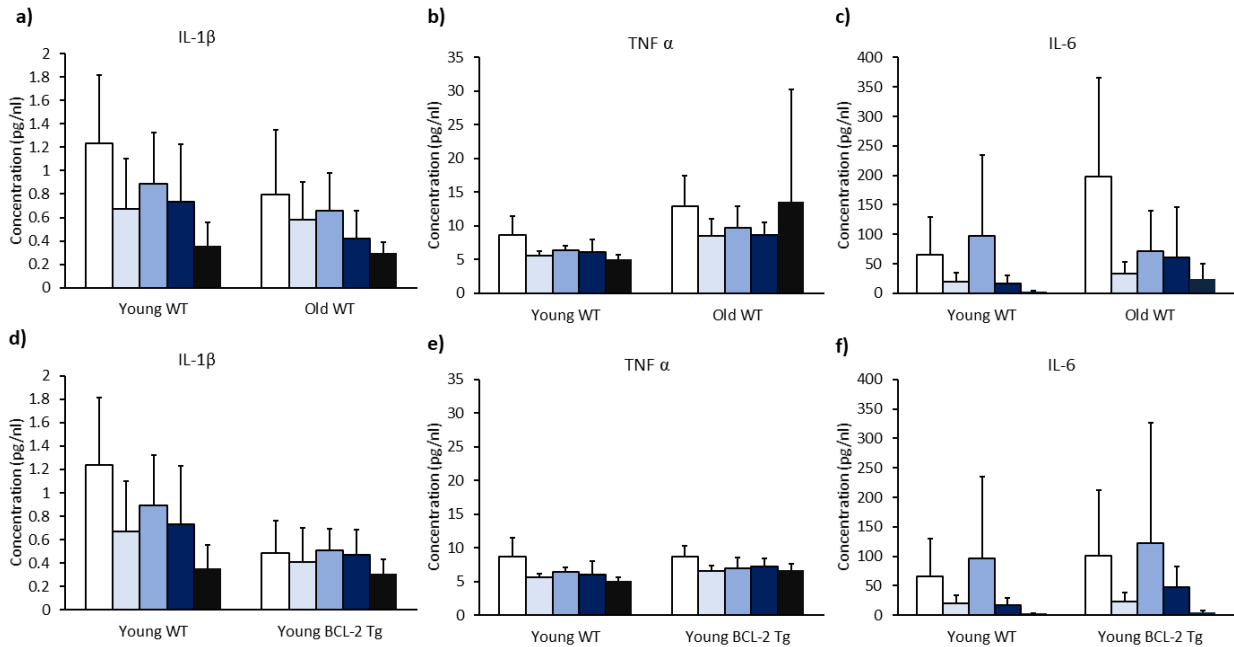


Figure 3.7: ELISA Results. Serum concentrations of IL-1 β (3.5a), TNF- α (3.5b), and IL-6 (3.5c) for Young WT, Old WT and Young BCL-2 Tg mice after 14 days of unloading followed by 14 days of reloading. Data are presented as means with standard deviations as error bars.

3.5 Discussion

In this study, our goal was to examine differences in bone adaptation in response to unloading and reloading between three different experimental groups of mice, Young WT, Old WT, and Young BCL-2 TG mice. We hypothesized that the bones of Young WT mice would have a more robust response to both unloading and reloading than the bones of Old WT mice, and that Young BCL-2 TG mice with high levels of osteocyte apoptosis would have a response similar to that of Old WT animals. Somewhat contrary to our hypothesis, Old WT mice had a robust bone adaptation response to unloading that was similar in effect size to Young WT animals. There were still key differences in bone adaptation between experimental groups, particularly in bone recovery during the

reloading period, but these differences were often site-specific and not as consistent as expected.

In Young WT mice, we observed significant trabecular bone loss in response to unloading in both trabecular bone sites, but far less cortical bone adaptation over the total time course of the study. While we observed recovery during reloading in epiphyseal trabecular bone of Young WT mice, we observed continued bone loss in the metaphyseal trabecular bone and cortical bone during reloading. There are a few potential causes for this continued bone loss during the reloading period. One potential explanation is that at the locations that we observed continued bone loss during reloading, it can take a significant period of time after the end of mechanical unloading to reverse unloading-induced bone resorption. Bone loss in the metaphysis during reloading occurred in early reloading while bone loss in the cortical diaphysis occurred in late reloading. Trabecular bone is a more dynamic tissue than cortical bone, and is far quicker to respond to changing mechanical loading environments^{50,133}; this could potentially explain the difference in timing of bone loss between the two sites during reloading. Another potential cause for bone loss during reloading could be that allowing a mouse to ambulate with its hindlimbs after 14 days of unloading could cause minor trauma to the bone from the sudden increase in mechanical loading. The mechanostat theory suggests that if strain magnitude in bone is above a certain threshold, bone accrues damage rather than just adapting with a net increase in bone mass^{21,24}. It is possible that due to unloading-induced bone loss compromising the structure of the bone, for a short period during early reloading, the strain magnitudes in newly reloaded bones may be high enough to accrue

some amount of damage, and this might be the initiating event for the bone loss that we observe in early reloading. In future work, it would be valuable to examine bone microdamage in newly reloaded bone samples through histology to determine if there is increased microdamage and how the amount of microdamage compares to microdamage in bone samples from subjects who underwent normal ambulation.

In cortical bone, the time delay between the change of mechanical loading and the bone adaptation response was even longer in Young WT mice than in the trabecular bone. Though the effect size was much smaller than in trabecular bone, our results suggest that, in Young WT mice, adaptation to mechanical unloading was not detectable until 14 days after tail suspension ended. Mechanical testing indicated similar trends in structural and material properties to the cortical bone properties. We observed a lower effect of unloading and reloading on cortical bone properties that we analyzed, but any changes we observed were still present after 14 days of reloading.

A previous study reported very little bone adaptation in old animals during a period of unloading¹⁰³. In our previous study in rats, we observed no significant decreases in trabecular bone during 14 days of unloading, and we observed no significant decreases in cortical bone in response to unloading or reloading¹²⁹. In the current study, we observed that at baseline, Old WT mice had lower osteocyte density and increased osteocyte apoptosis in the cortical bone than Young WT mice. With a lower osteocyte density and higher osteocyte apoptosis, we expected drastically lower bone adaptation in response

to any change in the mechanical loading environment, both unloading and reloading. Contrary to this hypothesis, Old WT mice experienced consistent bone loss in the distal epiphysis and the mid diaphysis of the femur following the unloading period and mild recovery of trabecular bone during the reloading period.

Trabecular bone loss in the epiphysis of Old WT mice was a similar magnitude as in Young WT mice. At the metaphysis, bone loss was less consistent across trabecular bone parameters. However, we found that there is very little trabecular bone remaining in mice at this age which agrees with previous studies examining bone in 18-month-old mice⁷⁹. Thus, with so little trabecular bone present, even small changes in individual trabeculae can greatly increase the variation of the subgroup, potentially making it more difficult to detect significant differences. Trabecular bone is maintained in the epiphysis with age, so at that location, trabecular bone loss was more consistent across subgroups. It is difficult to compare our results to previous studies as previous studies examining unloading in old animals have used rats and have generally not reported epiphyseal bone results. Nonetheless, we did observe that Old WT mice did respond differently than Young WT mice to reloading in the trabecular bone. While both ages of mice experienced some continued bone loss during early reloading, Old WT mice did not have the same magnitude of trabecular bone recovery after 14 days of reloading. Our hypothesis that Old WT mice would have diminished or no adaptation to both unloading and reloading proved to be not accurate, though we observed mildly diminished adaptation to reloading in trabecular bone Old WT mice.

In cortical bone, bone adaptation to unloading was quicker in Old WT mice than in Young WT mice. After the unloading period in Old WT mice, there was significant thinning of the cortical bone at the mid-diaphysis. Furthermore, there was a significant loss of cortical bone area after 2 days of reloading in Old WT mice which suggests a delayed effect of unloading on bone adaptation, even once unloading has ended. Mechanical testing of cortical bone revealed that unloading and reloading had the greatest effect on mechanical properties of bones from Old WT mice. Mechanical properties decreased significantly during the unloading period and some continued to decrease in reloading without significant recovery by 14 days of reloading. Significant decreases in multiple mechanical properties indicate that the strength of the bone was significantly compromised in Old WT mice following unloading and remained compromised for a long period after normal loading had resumed.

We used BCL-2 Tg mice in this study as a model of osteocyte dysfunction. At baseline, we observed that osteocyte density in cortical bone of Young BCL-2 Tg mice was comparable to Young WT mice (including both live and dead osteocytes), and osteocyte apoptosis was much higher in Young BCL-2 Tg mice. Since osteocytes are responsible for sensing and responding to mechanical loads in bone, high osteocyte apoptosis would suggest that Young BCL-2 Tg mice would have diminished bone adaptation in response to changing mechanical loading environments. A previous study showed that tail suspension in this BCL-2 Tg mouse model resulted in no significant trabecular bone loss in the metaphysis in response to unloading when the mice were 16 weeks old at the start of unloading⁵⁵. In our study of 12-week-old BCL-2 TG mice, we also

observed no significant loss of trabecular bone in the metaphysis during the unloading period. However, we observed bone loss in the epiphysis in response to unloading and in the metaphysis during early reloading.

Osteocyte density in the Young BCL-2 Tg mice was similar to that of Young WT mice, but bone adaptation to unloading and reloading was still affected. We previously observed that Old WT mice, who had both decreased osteocyte density and increased osteocyte apoptosis also had a difference in bone adaptation compared to Young WT mice. Since bone adaptation in Young BCL-2 Tg mice was affected, this suggests that an increase in osteocyte apoptosis alone is enough to impair bone's ability to respond to changes in mechanical loading environments. Previous studies have found that osteocyte apoptosis precedes disuse-induced bone loss^{60,62} and is localized to areas of microdamage in response to increased loading^{134,135}. While osteocyte apoptosis during reloading has not been directly measured, another study has modeled bone recovery during reloading using osteocyte viability based on the expected mechanical loading range that allows for osteocyte survival¹³⁶. In Young BCL-2 Tg mice, a lower number of alive osteocytes means that there are fewer osteocytes that can undergo apoptosis in response to either unloading or reloading which could impair bone adaptation. Further examination of the magnitude of osteocyte apoptosis in Young BCL-2 Tg mice during unloading and in all mice during reloading would be necessary to validate this theory.

Bone was lost in the epiphysis of the Young BCL-2 Tg mice at around the same magnitude as Young WT during unloading, but we observed no trabecular bone recovery during reloading. In the metaphysis, Young BCL-2 Tg mice lost bone in early reloading and this bone loss was not recovered after 14 days of reloading. Delayed trabecular bone loss in the metaphysis in response to disuse in Young BCL-2 Tg mice compared to the timing of trabecular bone loss in Young WT mice implies that trabecular bone at this site may be slower to adapt to a decreased mechanical loading environment in Young BCL-2 Tg mice than Young WT mice. The full time-course of bone recovery during reloading in Young BCL-2 Tg mice was not able to be determined due to the limited time scope of our study. However, the loss of trabecular bone structure during the early reloading period observed in μ CT analysis suggests a delay between return to normal loading and the start of bone recovery.

Cortical bone parameters in Young BCL-2 Tg mice did not respond at all to either unloading or reloading, and there were no differences observed in mechanical properties. Osteocyte death in the cortical bone in this transgenic mouse model has been observed to be around 50% at 10 weeks of age and 75% at 16 weeks of age^{55,131}. Though we only analyzed a limited number of samples, we observed osteocyte apoptosis at around 60% in 12-week-old BCL-2 Tg mice. Mechanoresponsiveness, particularly in the diaphysis of long bones, is thought to be heavily mediated by osteocytes^{26,130} and thus a lower osteocyte density and dysfunctional canalicular network in the Young BCL-2 Tg mice could explain the lack of cortical bone response to unloading and reloading in these mice.

As described earlier, the BCL-2 Tg mouse line that we used in this study was developed by the Komori lab in 2011 and in this transgenic mouse, human BCL-2 is overexpressed in osteoblasts and osteocytes under the control of the Col1a1(2.3kb) promoter¹³¹. However, this mouse line is not the first of its kind, a similar mouse line was developed by the Gronowicz lab in 2005 which also expresses human BCL-2 in osteoblasts and osteocytes under the control of the Col1a1(2.3kb) promoter¹³⁷. Tail suspension studies were not performed on the Gronowicz BCL-2 Tg mouse line so any differences in bone adaptation to disuse are not characterized.

Both mouse lines were extensively characterized but it is difficult to directly compare the Komori and Gronowicz lines as the characterization methods differed slightly and examined different time points though there are some overlapping time points. In the Gronowicz line, osteoblast and osteocyte apoptosis were measured at 8 weeks while in the Komori line, osteoblast apoptosis was measured at 2 and 6 weeks while osteocyte apoptosis was measured at 2, 4, 6 and 10 weeks. Osteoblast apoptosis was measured at different ages and was moderately higher in the Gronowicz BCL-2 Tg mouse, around 5-7% to the Komori BCL-2 Tg mouse's 2-4%. What differs significantly is osteocyte apoptosis between the two mice lines. At 8 weeks old, the Gronowicz mouse line had only about a 5% rate of osteocyte apoptosis¹³⁷ while between 6 and 10 weeks in the Komori line, osteocyte apoptosis increases from around 20% to around 50%¹³¹. In addition, the Gronowicz BCL-2 Tg mouse exhibits a high trabecular bone mass phenotype measured through histomorphometry at both 2 and 6 months of age¹³⁷ while the Komori BCL-2 Tg mouse exhibits a high bone mass phenotype at 4 weeks and 4 months of age

measured through μ CT⁵⁵. Though the Gronowicz BCL-2 Tg mouse has not been studied in tail suspension, without high osteocyte apoptosis, it is unlikely to have the same bone response to unloading and reloading that we observed in the Komori Young BCL-2 Tg mice.

The Komori BCL-2 transgenic mouse exhibits osteocyte dysfunction through a large increase in osteocyte apoptosis. Another transgenic mouse model modifies osteocyte function through targeted ablation. In this model established by Tatsumi et al., transgenic mice express the diphtheria toxin receptor (DT-R) under the control of the dentin matrix protein 1(DMP-1)¹³⁸. DMP-1 is highly expressed in osteocytes but not in osteoblasts, thus, in response to an injection of diphtheria toxin, around 50-70% of osteocytes undergo apoptosis or become necrotic. As the osteocyte ablation is an inducible effect, this mouse has no abnormal bone phenotype prior to the injection of DT. When this transgenic mouse underwent osteocyte ablation prior to 7 days of tail suspension, they did not experience unloading-induced bone loss. However, when osteocytes were instead ablated immediately following 7 days of tail suspension, mice experienced bone recovery during a reloading period¹³⁸. What is unclear about this mouse model is the nature by which the osteocytes are ablated. If the osteocytes undergo apoptosis, then if this process occurs immediately prior to tail suspension, one would expect there to be bone loss due to a large amount of osteocyte apoptosis which many studies suggest may trigger unloading induced bone loss^{60,62,64}. However, this does not occur suggesting that the circumstances of osteocyte apoptosis are important in determining the resulting bone adaptation response.

By comparison, in the Young BCL-2 Tg mice, a model with osteocytes that continuously undergo apoptosis, we observed no bone adaptation in cortical bone during unloading or reloading but we observed bone loss in response to unloading in trabecular bone. Differences in bone adaptation in response to unloading and reloading in these two mouse models might relate to the timing of osteocyte apoptosis in both models with the DT-inducible mouse experiencing one large wave of osteocyte apoptosis or death while the Kormori BCL-2 Tg experiences a continuous rate of osteocyte apoptosis. This could support the premise that it is not simply osteocyte apoptosis that regulates bone adaptation to disuse but the circumstances, including loading environment and outside cause of apoptosis, that regulate the response.

The magnitude and location of bone loss during unloading that we observed in Young WT mice is consistent with previous studies that examined slightly older mice (16-17 weeks old) over a similar unloading period in mice^{54,55}. In addition, though fewer studies have examined bone adaptation during reloading, these studies indicated that bone recovery in young animals takes longer than our 14-day reloading period^{50,52}, and thus it is reasonable that we did not observe complete recovery in our study. However, our results indicated a different pattern of bone adaptation than has previously been observed for tail suspension with old animals.

There are few studies that have examined the effect of disuse on the bones of old animals specifically, and these previous studies used ~28-month-old rats as a model,

whereas our study used 18-month-old mice. The old rats in these previous studies were older compared to their total life span than the old mice used in the current study, and this may explain some of the differences in bone adaptation that we observed in Old WT mice in this study versus previous studies in rats. Another factor that could contribute to the differences in adaptation effect size and timing could be the differences in basal metabolic rate between mice and rats. Mice have a significantly higher metabolic rate than rats do^{139,140}, which could mean that the same 14 day period of mechanical unloading could have a much larger effect on the more metabolically active mouse than the rat. Further research into age-related differences in bone adaptation in response to mechanical unloading and reloading is needed to clarify how and when bone adaptation changes with relative bone age.

Contrary to our initial hypotheses, all three experimental groups of mice lost bone during unloading, and all three experienced at least some continued loss of bone during early reloading. Young WT mice appeared to experience near complete bone recovery during reloading than Old WT mice, which experienced minimal recovery, and Young BCL-2 Tg mice, which effectively exhibited no recovery. High variance in serum levels of inflammatory cytokines within subgroups made it difficult to detect meaningful differences in serum cytokine levels over the course of unloading and reloading. In Old WT mice, TNF- α levels in serum were higher overall than Young WT and Young BCL-2 TG mice. Circulating inflammatory cytokine levels are higher in older subjects⁹⁹. This has been implicated as a possible contributing mechanism to the imbalance of bone formation and bone resorption that contributes to osteoporotic bone in older subjects⁸⁰. This difference

in circulating inflammatory cytokines could contribute to rapid bone loss in response to unloading seen in Old WT mice and could also contribute to diminished recovery of bone with reloading. However, further analyses examining inflammation in the potentially affected bone tissue, would be necessary to confirm this link. Potential analyses could include measuring local inflammatory cytokines in the surrounding tissue through ELISA, quantification of local expression of inflammatory cytokines through quantitative polymerase chain reaction or measuring changes in bone resorption through histology. Furthermore, the circulating cytokine levels that we measured do not indicate any significant differences between Young WT mice and Young BCL-2 Tg mice and therefore do not explain the differences in bone adaptation between these two experimental groups of mice.

There are several limitations to this study that affect our conclusions. This study is cross-sectional with multiple terminal time points; there are no analyses that captured the changes over the course of the unloading and reloading for any individual animal. In addition, prior to tail suspension, mice were group housed. After the unloading period, mice remained single housed during reloading, and may not have had the same level of activity as they had prior to the tail suspension due to the single housing. In addition, this study is limited in the conclusions it can draw mechanistically. Our analysis presents a thorough examination of structural and mechanical changes in response to loading and unloading, but mechanistically we only examined TUNEL staining of baseline samples and serum levels of three inflammatory cytokines throughout the study. Thus, while we have observed complex differences in site-specific bone adaptation between the three

experimental groups, we cannot currently determine what biological mechanisms caused these changes.

3.6 Conclusions

Despite some limitations, this study builds on previous work done by our lab examining age-related differences in bone adaptation in response to mechanical unloading and subsequent reloading. In this study, Old mice experienced significant trabecular and cortical bone loss in response to unloading. However, we observed a significant delay in bone recovery and additional bone loss in early reloading which further indicates that there is a window of skeletal vulnerability in older subjects following a period of disuse. Using a transgenic model of osteocyte dysfunction, we observed that in these mice, bone loss occurs only in trabecular bone and does not recover during the short time period that we examined. Impaired bone adaptation, particularly in cortical bone suggests that osteocyte apoptosis or osteocyte dysfunction has a significant effect on bone's response to changing mechanical loading environments. This research motivates further investigations into specific differences in bone adaptation based on age and other factors to better preserve the skeletal health of elderly patients following significant periods of bedrest or disuse.

Chapter 4: Conclusions and Future Directions

Maintaining skeletal health is an important health concern for elderly patients. However, the specific risk posed by periods of disuse and subsequent recovery to skeletal health in older subjects has received relatively little investigation. In this research, we demonstrated that bone adaptation in old animals to mechanical unloading and subsequent reloading is different to that of young animals.

In the first study, we observed that old rats (equivalent to a 70-80 year old human) did not lose bone during mechanical unloading but did lose significant trabecular bone during the subsequent reloading period. This trabecular bone loss was not recovered and did not even begin to recover after 28 days of reloading. The unloading response in old rats is consistent with what has been observed in a previous study¹⁰³ however, the continued loss during reloading has not been seen before. This research potentially implies that, in old subjects, the time needed to reverse bone resorption due to disuse and begin bone formation is extended and leaves the subject in a vulnerable state of skeletal health.

In the second study, we observed that old mice (equivalent to a 50-60 year old human) lost amounts of cortical and trabecular bone during unloading. In addition, further bone loss during early reloading was observed and old mice experienced significantly less bone recovery during the study timeline than young mice. While the bone adaptation of the Old mice differed from the Young mice, the results in this study

were different than what has been observed in old rats. In past studies, bones of old rats did not lose bone during a 14 day bout of tail suspension¹⁰³ while in our study, we observed bone loss during a return to normal loading¹²⁹. Some of the differences might be due to the different relative ages of the two old animals which illustrates the need for research into how bone adaptation changes at several points in aging.

In the second study we also observed the effect of unloading and reloading on bone adaptation in Young BCL-2 Tg mice who display increased osteocyte apoptosis. Young BCL-2 mice exhibited no cortical bone adaptation to either unloading or reloading and displayed minimal recovery in trabecular bone parameters during reloading. Increased osteocyte apoptosis could have affected the bone's ability to sense and respond to changing mechanical loading environments^{95,130}.

However, though we did not directly compare them, Young BCL-2 Tg mice and Old WT mice did not have the same bone adaptation response to unloading and reloading even though both had high osteocyte apoptosis. Old WT mice also had a diminished osteocyte density but still had a robust bone adaptation response to unloading. Osteocyte apoptosis is heavily associated with the initial bone loss during unloading^{62,64} and it is possible that with fewer live osteocyte to undergo apoptosis in Young BCL-2 Tg and Old WT mice, it may impair bone adaptation. However, this does not explain why the response was different between the two. Osteocyte apoptosis has also been observed in response to increased loading of bone at sites of microdamage

caused by the increased loading^{134,135} which is a response would likely occur in osteocytes during reloading which has been modeled¹³⁶ but has not been directly measured in previous studies. Again, if more osteocytes have already undergone apoptosis, there would be fewer remaining to undergo apoptosis in response to reloading and if this signal is necessary to trigger bone remodeling, then bone remodeling would be impaired. There also may be other factors beyond osteocyte density and osteocyte apoptosis that regulate bone's response to changing mechanical loading environment. Further investigation into osteocyte apoptosis during unloading and reloading would be required to fully understand why these bone adaptation response in Young BCL-2 Tg mice and Old WT mice differed.

In our tail suspension study in mice, we observed that trabecular bone continued to decrease during early reloading. This further validates the concept observed in spaceflight studies wherein it takes several days of normal mechanical loading before the bone resorption due to disuse is reversed, even in young subjects^{41,44}.

The major limitations of this research are in the cross-sectional study design and the lack of mechanistic analysis. Both studies are cross-sectional and thus bone adaptation in a single subject cannot be captured and bone loss and recovery are implied between groups. It would be valuable to capture bone adaptation across individual animals to validate what has been seen in our cross-sectional studies.

The second major weakness of this research is the lack of mechanistic analyses which limits the conclusions that can be drawn. In the first study, we did not have any mechanistic analyses. In the second study, mechanistic analyses were limited. We measured circulating inflammatory cytokines in the serum of the mice, and we observed differences in osteocyte density and osteocyte apoptosis at baseline using TUNEL staining. The analysis of circulating inflammatory cytokines did not uncover any differences in response to unloading or reloading and the TUNEL staining allowed us to see differences between mouse experimental groups at baseline but did not examine adaptation during the study. Future work on this project will involve an expansion of mechanistic analyses so that we can analyze differences in bone adaptation beyond structural changes observed. Future analyses will include an expansion of TUNEL staining analysis to examine changes in osteocyte apoptosis during unloading and reloading within each experimental group of mice, and qPCR to examine changes in local gene expression affecting inflammation, bone resorption and bone formation during unloading and reloading.

Another potential effect of bone adaptation to disuse that we did not examine in these studies was cortical porosity. Cortical porosity increase in bones with age^{8,123}. In addition, some spaceflight studies have found an increase in cortical porosity in response to mechanical unloading⁴⁵. Increasing cortical porosity has a negative effect on the mechanical strength of the bone and quantifying cortical porosity changes with disuse would be valuable to further understand potential windows of skeletal

vulnerability during which elderly patients may be more vulnerable to musculoskeletal injury.

Overall, this research demonstrates that there are differences in bone adaptation in response to mechanical unloading and subsequent reloading as a function of age. This research adds to the limited number of studies examining bone adaptation in aged subjects. It further highlights potential skeletal vulnerabilities in not only old patients but young as well. This research has the potential to motivate further research into bone adaptation in older subjects to further understand potential vulnerabilities to skeletal health in elderly patients.

References

1. Kanis, J. A., Melton III, L. J., Christiansen, C., Johnston, C. C. & Khaltaev, N. The diagnosis of osteoporosis. *J. Bone Miner. Res.* **9**, 1137–1141 (1994).
2. Osteoporosis Fast Facts. *National Osteoporosis Foundation* <https://cdn.nof.org/wp-content/uploads/2015/12/Osteoporosis-Fast-Facts.pdf> (2015).
3. Silva, T. J. A., Jerussalmy, C. S., Farfel, J. M., Curiati, J. A. E. & Jacob-Filho, W. Predictors of in-hospital mortality among older patients. *Clinics (Sao Paulo)*. **64**, 613–618 (2009).
4. Czaja, C. A. *et al.* Age-Related Differences in Hospitalization Rates, Clinical Presentation, and Outcomes Among Older Adults Hospitalized With Influenza- U.S. Influenza Hospitalization Surveillance Network (FluSurv-NET). *Open forum Infect. Dis.* **6**, (2019).
5. Russo, A. & Elixhauser, A. *Hospitalizations in the Elderly Population, 2003*. <https://www.hcup-us.ahrq.gov/reports/statbriefs/sb6.pdf> (2003).
6. Martin, B., Burr, D., Sharkey, N. & Fyhrie, D. *Skeletal Tissue Mechanics*. (Springer, 2015).
7. Seref-Ferlengez, Z., Kennedy, O. D. & Schaffler, M. B. Bone microdamage, remodeling and bone fragility: how much damage is too much damage? *Bonekey Rep.* **4**, 644 (2015).
8. Goltzman, D. The Aging Skeleton BT - Human Cell Transformation: Advances in Cell Models for the Study of Cancer and Aging. in (eds. Rhim, J. S., Dritschilo, A. & Kremer, R.) 153–160 (Springer International Publishing, 2019). doi:10.1007/978-3-030-22254-3_12.
9. HADJIDAKIS, D. J. & ANDROULAKIS, I. I. Bone Remodeling. *Ann. N. Y. Acad. Sci.* **1092**, 385–396 (2006).
10. Raggatt, L. J. & Partridge, N. C. Cellular and Molecular Mechanisms of Bone Remodeling. *J. Biol. Chem.* **285**, 25103–25108 (2010).
11. Delgado-Calle, J. & Bellido, T. Basic Aspects of Osteocyte Function BT - Osteoporosis: Pathophysiology and Clinical Management. in (eds. Leder, B. Z. & Wein, M. N.) 43–69 (Springer International Publishing, 2020). doi:10.1007/978-3-319-69287-6_3.
12. Baron, R. & Kneissel, M. WNT signaling in bone homeostasis and disease: from human mutations to treatments. *Nat. Med.* **19**, 179–192 (2013).
13. Gasser, J. & Kneissel, M. Bone Physiology and Biology. in 27–94 (2017). doi:10.1007/978-3-319-56192-9_2.
14. Eriksen, E. F. Normal and Pathological Remodeling of Human Trabecular Bone:

- Three Dimensional Reconstruction of the Remodeling Sequence in Normals and in Metabolic Bone Disease*. *Endocr. Rev.* **7**, 379–408 (1986).
15. Eriksen, E. F., Gundersen, H. J. G., Melsen, F. & Mosekilde, L. Reconstruction of the formative site in iliac trabecular bone in 20 normal individuals employing a kinetic model for matrix and mineral apposition. *Metab. Bone Dis. Relat. Res.* **5**, 243–252 (1984).
 16. Jilka, R. L. The relevance of mouse models for investigating age-related bone loss in humans. *J. Gerontol. A. Biol. Sci. Med. Sci.* **68**, 1209–1217 (2013).
 17. Weinstein, R. S., Jilka, R. L., Parfitt, A. M. & Manolagas, S. C. Inhibition of osteoblastogenesis and promotion of apoptosis of osteoblasts and osteocytes by glucocorticoids. Potential mechanisms of their deleterious effects on bone. *J. Clin. Invest.* **102**, 274–282 (1998).
 18. Baron, R. Remaniement de l'os alvéolaire et des fibres desmodontales au cours de la migration physiologique. *J. Biol. buccale* **1**, 151–170 (1973).
 19. Baron, R., Tross, R. & Vignery, A. Evidence of sequential remodeling in rat trabecular bone: Morphology, dynamic histomorphometry, and changes during skeletal maturation. *Anat. Rec.* **208**, 137–145 (1984).
 20. Robling, A. G., Castillo, A. B. & Turner, C. H. BIOMECHANICAL AND MOLECULAR REGULATION OF BONE REMODELING. *Annu. Rev. Biomed. Eng.* **8**, 455–498 (2006).
 21. Cowin, S. C. Wolff's Law of Trabecular Architecture at Remodeling Equilibrium. *J. Biomech. Eng.* **108**, 83–88 (1986).
 22. Frost, H. M. Perspectives: A proposed general model of the “mechanostat” (suggestions from a new skeletal-biologic paradigm). *Anat. Rec.* **244**, 139–147 (1996).
 23. Frost, H. M. Bone's mechanostat: A 2003 update. *Anat. Rec. Part A Discov. Mol. Cell. Evol. Biol.* **275A**, 1081–1101 (2003).
 24. Frost, H. M. The Utah paradigm of skeletal physiology: an overview of its insights for bone, cartilage and collagenous tissue organs. *J. Bone Miner. Metab.* **18**, 305–316 (2000).
 25. Yavropoulou, M. P. & Yovos, J. G. The molecular basis of bone mechanotransduction. *J. Musculoskelet. Neuronal Interact.* **16**, 221–236 (2016).
 26. Piekarski, K. & Munro, M. Transport mechanism operating between blood supply and osteocytes in long bones. *Nature* **269**, 80–82 (1977).
 27. Wang, L. *et al.* In situ measurement of solute transport in the bone lacunar-canalicular system. *Proc. Natl. Acad. Sci. U. S. A.* **102**, 11911–11916 (2005).
 28. Burra, S. *et al.* Dendritic processes of osteocytes are mechanotransducers that induce the opening of hemichannels. *Proc. Natl. Acad. Sci. U. S. A.* **107**, 13648–

- 13653 (2010).
29. Wang, Y., McNamara, L. M., Schaffler, M. B. & Weinbaum, S. A model for the role of integrins in flow induced mechanotransduction in osteocytes. *Proc. Natl. Acad. Sci. U. S. A.* **104**, 15941–15946 (2007).
 30. Plotkin, L. I. Apoptotic osteocytes and the control of targeted bone resorption. *Curr. Osteoporos. Rep.* **12**, 121–126 (2014).
 31. Siddiqui, J. A. & Partridge, N. C. Physiological Bone Remodeling: Systemic Regulation and Growth Factor Involvement. *Physiology* **31**, 233–245 (2016).
 32. LeBlanc, A. *et al.* Bone mineral and lean tissue loss after long duration space flight. *J. Musculoskelet. Neuronal Interact.* **1**, 157–160 (2000).
 33. Ohshima, H. [Bone loss and bone metabolism in astronauts during long-duration space flight]. *Clin. Calcium* **16**, 81–85 (2006).
 34. Jee, W. S., Wronski, T. J., Morey, E. R. & Kimmel, D. B. Effects of spaceflight on trabecular bone in rats. *Am. J. Physiol. Integr. Comp. Physiol.* **244**, R310–R314 (1983).
 35. Stein, T. P. Weight, muscle and bone loss during space flight: another perspective. *Eur. J. Appl. Physiol.* **113**, 2171–2181 (2013).
 36. Keyak, J. H., Koyama, A. K., LeBlanc, A., Lu, Y. & Lang, T. F. Reduction in proximal femoral strength due to long-duration spaceflight. *Bone* **44**, 449–453 (2009).
 37. Beller, G. *et al.* WISE-2005: bed-rest induced changes in bone mineral density in women during 60 days simulated microgravity. *Bone* **49**, 858–866 (2011).
 38. Leblanc, A. D., Schneider, V. S., Evans, H. J., Engelbretson, D. A. & Krebs, J. M. Bone mineral loss and recovery after 17 weeks of bed rest. *J. Bone Miner. Res.* **5**, 843–850 (1990).
 39. Lloyd, S. A. *et al.* Osteoprotegerin is an effective countermeasure for spaceflight-induced bone loss in mice. *Bone* **81**, 562–572 (2015).
 40. Berg-Johansen, B. *et al.* Spaceflight-induced bone loss alters failure mode and reduces bending strength in murine spinal segments. *J. Orthop. Res.* **34**, 48–57 (2016).
 41. Gerbaix, M. *et al.* Eight Days of Earth Reambulation Worsen Bone Loss Induced by 1-Month Spaceflight in the Major Weight-Bearing Ankle Bones of Mature Mice. *Front. Physiol.* **9**, 746 (2018).
 42. Carmeliet, G., Vico, L. & Bouillon, R. Space flight: A challenge for normal bone homeostasis. *Critical Reviews in Eukaryotic Gene Expression* vol. 11 131–144 (2001).
 43. Wronski, T. J. & Morey, E. R. Effect of spaceflight on periosteal bone formation in rats. *Am. J. Physiol.* **244**, R305-9 (1983).

44. Gerbaix, M. *et al.* One-month spaceflight compromises the bone microstructure, tissue-level mechanical properties, osteocyte survival and lacunae volume in mature mice skeletons. *Sci. Rep.* **7**, 2659 (2017).
45. Maupin, K. A. *et al.* Skeletal adaptations in young male mice after 4 weeks aboard the International Space Station. *NPJ microgravity* **5**, 21 (2019).
46. Keune, J. A., Philbrick, K. A., Branscum, A. J., Iwaniec, U. T. & Turner, R. T. Spaceflight-induced vertebral bone loss in ovariectomized rats is associated with increased bone marrow adiposity and no change in bone formation. *NPJ microgravity* **2**, 16016 (2016).
47. Marzuca-Nassr, G. *et al.* Acute Electrical Stimulation Modifies Cross-sectional Area and Desmin Protein in the Skeletal Muscle of Old Rats Submitted to Hindlimb Suspension. *Indian J. Physiol. Pharmacol.* **61**, 219 (2017).
48. Wronski, T. J. & Morey-Holton, E. R. Skeletal response to simulated weightlessness: a comparison of suspension techniques. *Aviat. Space. Environ. Med.* **58**, 63–68 (1987).
49. Morey-Holton, E. R. & Globus, R. K. Hindlimb unloading of growing rats: a model for predicting skeletal changes during space flight. *Bone* **22**, 83S-88S (1998).
50. Basso, N., Jia, Y., Bellows, C. G. & Heersche, J. N. M. The effect of reloading on bone volume, osteoblast number, and osteoprogenitor characteristics: studies in hind limb unloaded rats. *Bone* **37**, 370–378 (2005).
51. David, V. *et al.* Two-week longitudinal survey of bone architecture alteration in the hindlimb-unloaded rat model of bone loss: sex differences. *Am. J. Physiol. Endocrinol. Metab.* **290**, E440-7 (2006).
52. Shirazi-Fard, Y. *et al.* Previous exposure to simulated microgravity does not exacerbate bone loss during subsequent exposure in the proximal tibia of adult rats. *Bone* **56**, 461–473 (2013).
53. Bloomfield, S. A., Allen, M. R., Hogan, H. A. & Delp, M. D. Site- and compartment-specific changes in bone with hindlimb unloading in mature adult rats. *Bone* **31**, 149–157 (2002).
54. Amblard, D. *et al.* Tail Suspension Induces Bone Loss in Skeletally Mature Mice in the C57BL/6J Strain but Not in the C3H/HeJ Strain. *J. Bone Miner. Res.* **18**, 561–569 (2003).
55. Moriishi, T. *et al.* Osteocyte network; a negative regulatory system for bone mass augmented by the induction of Rankl in osteoblasts and Sost in osteocytes at unloading. *PLoS One* **7**, e40143–e40143 (2012).
56. Colaianni, G. *et al.* Irisin prevents and restores bone loss and muscle atrophy in hind-limb suspended mice. *Sci. Rep.* **7**, 2811 (2017).
57. Xu, Z. *et al.* The regulation of iron metabolism by hepcidin contributes to unloading-induced bone loss. *Bone* **94**, 152–161 (2017).

58. Sankaran, J. S., Varshney, M. & Judex, S. Differences in bone structure and unloading-induced bone loss between C57BL/6N and C57BL/6J mice. *Mamm. Genome* **28**, 476–486 (2017).
59. Judex, S. *et al.* Genetically Linked Site-Specificity of Disuse Osteoporosis. *J. Bone Miner. Res.* **19**, 607–613 (2004).
60. Aguirre, J. I. *et al.* Osteocyte Apoptosis Is Induced by Weightlessness in Mice and Precedes Osteoclast Recruitment and Bone Loss. *J. Bone Miner. Res.* **21**, 605–615 (2006).
61. Lloyd, S. A. *et al.* Effect of proton irradiation followed by hindlimb unloading on bone in mature mice: A model of long-duration spaceflight. *Bone* **51**, 756–764 (2012).
62. Kennedy, O. D., Laudier, D. M., Majeska, R. J., Sun, H. B. & Schaffler, M. B. Osteocyte apoptosis is required for production of osteoclastogenic signals following bone fatigue in vivo. *Bone* **64**, 132–137 (2014).
63. Kennedy, O. D. *et al.* Activation of resorption in fatigue-loaded bone involves both apoptosis and active pro-osteoclastogenic signaling by distinct osteocyte populations. *Bone* **50**, 1115–1122 (2012).
64. Cabahug-Zuckerman, P. *et al.* Osteocyte Apoptosis Caused by Hindlimb Unloading is Required to Trigger Osteocyte RANKL Production and Subsequent Resorption of Cortical and Trabecular Bone in Mice Femurs. *J. Bone Miner. Res.* **31**, 1356–1365 (2016).
65. Plotkin, L. I. *et al.* Inhibition of osteocyte apoptosis prevents the increase in osteocytic receptor activator of nuclear factor κ B ligand (RANKL) but does not stop bone resorption or the loss of bone induced by unloading. *J. Biol. Chem.* **290**, 18934–18942 (2015).
66. Lang, T. F., Leblanc, A. D., Evans, H. J. & Lu, Y. Adaptation of the Proximal Femur to Skeletal Reloading After Long-Duration Spaceflight. *J. Bone Miner. Res.* **21**, 1224–1230 (2006).
67. Shirazi-Fard, Y. *et al.* Moderate intensity resistive exercise improves metaphyseal cancellous bone recovery following an initial disuse period, but does not mitigate decrements during a subsequent disuse period in adult rats. *Bone* **66**, 296–305 (2014).
68. Sakai, A. & Nakamura, T. Changes in trabecular bone turnover and bone marrow cell development in tail-suspended mice. *J. Musculoskelet. Neuronal Interact.* **1**, 387–392 (2001).
69. Allen, M. R., Hogan, H. A. & Bloomfield, S. A. Differential bone and muscle recovery following hindlimb unloading in skeletally mature male rats. *J. Musculoskelet. Neuronal Interact.* **6**, 217–225 (2006).
70. Mori, S. [Aging and homeostasis. Aging of bone.]. *Clin. Calcium* **27**, 917–923 (2017).

71. Wei, Y. & Sun, Y. Aging of the Bone BT - Aging and Aging-Related Diseases: Mechanisms and Interventions. in (ed. Wang, Z.) 189–197 (Springer Singapore, 2018). doi:10.1007/978-981-13-1117-8_12.
72. Burr, D. B. Muscle strength, bone mass, and age-related bone loss. *J. bone Miner. Res. Off. J. Am. Soc. Bone Miner. Res.* **12**, 1547–1551 (1997).
73. Khosla, S., Melton, L. J. 3rd & Riggs, B. L. Osteoporosis: gender differences and similarities. *Lupus* **8**, 393–396 (1999).
74. Manolagas, S. C. & Parfitt, A. M. What old means to bone. *Trends Endocrinol. Metab.* **21**, 369–374 (2010).
75. Ding, M. & Hvid, I. Quantification of age-related changes in the structure model type and trabecular thickness of human tibial cancellous bone. *Bone* **26**, 291–295 (2000).
76. Halloran, B. P. *et al.* Changes in Bone Structure and Mass With Advancing Age in the Male C57BL/6J Mouse. *J. Bone Miner. Res.* **17**, 1044–1050 (2002).
77. Mosekilde, L. Sex differences in age-related loss of vertebral trabecular bone mass and structure—biomechanical consequences. *Bone* **10**, 425–432 (1989).
78. Majumdar, S. *et al.* Correlation of Trabecular Bone Structure with Age, Bone Mineral Density, and Osteoporotic Status: In Vivo Studies in the Distal Radius Using High Resolution Magnetic Resonance Imaging. *J. Bone Miner. Res.* **12**, 111–118 (1997).
79. Glatt, V., Canalis, E., Stadmeier, L. & Bouxsein, M. L. Age-Related Changes in Trabecular Architecture Differ in Female and Male C57BL/6J Mice. *J. Bone Miner. Res.* **22**, 1197–1207 (2007).
80. Gibon, E., Lu, L. & Goodman, S. B. Aging, inflammation, stem cells, and bone healing. *Stem Cell Res. Ther.* **7**, 44 (2016).
81. Nyman, J. S. *et al.* Age-related effect on the concentration of collagen crosslinks in human osteonal and interstitial bone tissue. *Bone* **39**, 1210–1217 (2006).
82. Oxlund, H., Sekilde, L. & Ørtoft, G. Reduced concentration of collagen reducible cross links in human trabecular bone with respect to age and osteoporosis. *Bone* **19**, 479–484 (1996).
83. Burstein, A. H., Reilly, D. T. & Martens, M. Aging of bone tissue: mechanical properties. *J. Bone Joint Surg. Am.* **58**, 82–86 (1976).
84. Chung, P.-L. *et al.* Effect of Age on Regulation of Human Osteoclast Differentiation. *J. Cell. Biochem.* **115**, 1412–1419 (2014).
85. Jilka, R. L., Weinstein, R. S., Parfitt, A. M. & Manolagas, S. C. Quantifying osteoblast and osteocyte apoptosis: challenges and rewards. *J. bone Miner. Res. Off. J. Am. Soc. Bone Miner. Res.* **22**, 1492–1501 (2007).
86. Polster, B. M. & Fiskum, G. Mitochondrial mechanisms of neural cell apoptosis. *J.*

- Neurochem.* **90**, 1281–1289 (2004).
87. Zhou, S. *et al.* Age-related intrinsic changes in human bone-marrow-derived mesenchymal stem cells and their differentiation to osteoblasts. *Aging Cell* **7**, 335–343 (2008).
 88. Roholl, P. J., Blauw, E., Zurcher, C., Dormans, J. A. & Theuns, H. M. Evidence for a diminished maturation of preosteoblasts into osteoblasts during aging in rats: an ultrastructural analysis. *J. bone Miner. Res. Off. J. Am. Soc. Bone Miner. Res.* **9**, 355–366 (1994).
 89. Kassem, M. & Marie, P. J. Senescence-associated intrinsic mechanisms of osteoblast dysfunctions. *Aging Cell* **10**, 191–197 (2011).
 90. Mullender, M. G., van der Meer, D. D., Huiskes, R. & Lips, P. Osteocyte density changes in aging and osteoporosis. *Bone* **18**, 109–113 (1996).
 91. Jilka, R. L. & O'Brien, C. A. The Role of Osteocytes in Age-Related Bone Loss. *Curr. Osteoporos. Rep.* **14**, 16–25 (2016).
 92. Lai, X. *et al.* The dependences of osteocyte network on bone compartment, age, and disease. *Bone Res.* **3**, 15009 (2015).
 93. Noble, B. S., Stevens, H., Loveridge, N. & Reeve, J. Identification of apoptotic changes in osteocytes in normal and pathological human bone. *Bone* **20**, 273–282 (1997).
 94. Busse, B. *et al.* Decrease in the osteocyte lacunar density accompanied by hypermineralized lacunar occlusion reveals failure and delay of remodeling in aged human bone. *Aging Cell* **9**, 1065–1075 (2010).
 95. Vashishth, D., Verborgt, O., Divine, G., Schaffler, M. B. & Fyhrie, D. P. Decline in osteocyte lacunar density in human cortical bone is associated with accumulation of microcracks with age. *Bone* **26**, 375–380 (2000).
 96. Lavin, K. M. *et al.* Effects of aging and lifelong aerobic exercise on basal and exercise-induced inflammation. *J. Appl. Physiol.* **128**, 87–99 (2019).
 97. Franceschi, C. *et al.* Inflamm-aging: An Evolutionary Perspective on Immunosenescence. *Ann. N. Y. Acad. Sci.* **908**, 244–254 (2000).
 98. Ferrucci, L. *et al.* The origins of age-related proinflammatory state. *Blood* **105**, 2294–2299 (2005).
 99. Stranks, A. J. *et al.* Autophagy Controls Acquisition of Aging Features in Macrophages. *J. Innate Immun.* **7**, 375–391 (2015).
 100. Gómez, C. R. *et al.* Serum from aged F344 rats conditions the activation of young macrophages. *Mech. Ageing Dev.* **127**, 257–263 (2006).
 101. Collet, P. *et al.* Effects of 1- and 6-month spaceflight on bone mass and biochemistry in two humans. *Bone* **20**, 547–551 (1997).

102. Lang, T. *et al.* Cortical and trabecular bone mineral loss from the spine and hip in long-duration spaceflight. *J. bone Miner. Res. Off. J. Am. Soc. Bone Miner. Res.* **19**, 1006–1012 (2004).
103. Perrien, D. S. *et al.* Aging alters the skeletal response to disuse in the rat. *Am. J. Physiol. Integr. Comp. Physiol.* **292**, R988–R996 (2007).
104. Durbin, S. M. *et al.* Resveratrol supplementation preserves long bone mass, microstructure, and strength in hindlimb-suspended old male rats. *J. Bone Miner. Metab.* **32**, 38–47 (2014).
105. Bikle, D. D. & Halloran, B. P. The response of bone to unloading. *J. Bone Miner. Metab.* **17**, 233–244 (1999).
106. Rubin, C. T., Bain, S. D. & McLeod, K. J. Suppression of the osteogenic response in the aging skeleton. *Calcif. Tissue Int.* **50**, 306–313 (1992).
107. Holguin, N., Brodt, M. D., Sanchez, M. E. & Silva, M. J. Aging diminishes lamellar and woven bone formation induced by tibial compression in adult C57BL/6. *Bone* **65**, 83–91 (2014).
108. Vico, L. *et al.* Effects of long-term microgravity exposure on cancellous and cortical weight-bearing bones of cosmonauts. *Lancet (London, England)* **355**, 1607–1611 (2000).
109. Shirazi-Fard, Y., Kupke, J. S., Bloomfield, S. A. & Hogan, H. A. Discordant recovery of bone mass and mechanical properties during prolonged recovery from disuse. *Bone* **52**, 433–443 (2013).
110. Kortebein, P., Ferrando, A., Lombeida, J., Wolfe, R. & Evans, W. J. Effect of 10 days of bed rest on skeletal muscle in healthy older adults. *JAMA* vol. 297 1772–1774 (2007).
111. English, K. L. & Paddon-Jones, D. Protecting muscle mass and function in older adults during bed rest. *Curr. Opin. Clin. Nutr. Metab. Care* **13**, 34–39 (2010).
112. Weinreb, M., Rodan, G. A. & Thompson, D. D. Osteopenia in the immobilized rat hind limb is associated with increased bone resorption and decreased bone formation. *Bone* **10**, 187–194 (1989).
113. Maeda, H., Kimmel, D. B., Raab, D. M. & Lane, N. E. Musculoskeletal recovery following hindlimb immobilization in adult female rats. *Bone* **14**, 153–159 (1993).
114. Beaupied, H. *et al.* The mode of bone conservation does not affect the architecture and the tensile properties of rat femurs. *Biomed. Mater. Eng.* **16**, 253–259 (2006).
115. Linde, F. & Sørensen, H. C. The effect of different storage methods on the mechanical properties of trabecular bone. *J. Biomech.* **26**, 1249–1252 (1993).
116. Hogan, H. A., Ruhmann, S. P. & Sampson, H. W. The mechanical properties of cancellous bone in the proximal tibia of ovariectomized rats. *J. bone Miner. Res.*

- Off. J. Am. Soc. Bone Miner. Res.* **15**, 284–292 (2000).
117. Baehr, L. M. *et al.* Age-related deficits in skeletal muscle recovery following disuse are associated with neuromuscular junction instability and ER stress, not impaired protein synthesis. *Aging (Albany, NY)*. **8**, 127–146 (2016).
 118. Zerwekh, J. E., Ruml, L. A., Gottschalk, F. & Pak, C. Y. The effects of twelve weeks of bed rest on bone histology, biochemical markers of bone turnover, and calcium homeostasis in eleven normal subjects. *J. bone Miner. Res. Off. J. Am. Soc. Bone Miner. Res.* **13**, 1594–1601 (1998).
 119. Inoue, M. *et al.* Altered biochemical markers of bone turnover in humans during 120 days of bed rest. *Bone* **26**, 281–286 (2000).
 120. Globus, R. K., Bikle, D. D. & Morey-Holton, E. The temporal response of bone to unloading. *Endocrinology* **118**, 733–742 (1986).
 121. Stabley, J. N., Prisby, R. D., Behnke, B. J. & Delp, M. D. Chronic skeletal unloading of the rat femur: mechanisms and functional consequences of vascular remodeling. *Bone* **57**, 355–360 (2013).
 122. Akkus, O., Adar, F. & Schaffler, M. B. Age-related changes in physicochemical properties of mineral crystals are related to impaired mechanical function of cortical bone. *Bone* **34**, 443–453 (2004).
 123. Danielsen, C. C., Mosekilde, L. & Svenstrup, B. Cortical bone mass, composition, and mechanical properties in female rats in relation to age, long-term ovariectomy, and estrogen substitution. *Calcif. Tissue Int.* **52**, 26–33 (1993).
 124. Seeman, E. Pathogenesis of bone fragility in women and men. *Lancet* **359**, 1841–1850 (2002).
 125. Turner, C. H. Bone strength: current concepts. *Ann. N. Y. Acad. Sci.* **1068**, 429–446 (2006).
 126. Komori, T. Mouse models for the evaluation of osteocyte functions. *J. bone Metab.* **21**, 55–60 (2014).
 127. Parfitt, A. M. Bone age, mineral density, and fatigue damage. *Calcif. Tissue Int.* **53**, S82–S86 (1993).
 128. Daley, M. J. & Spinks, W. L. Exercise, Mobility and Aging. *Sport. Med.* **29**, 1–12 (2000).
 129. Cunningham, H. C. *et al.* Age-dependent bone loss and recovery during hindlimb unloading and subsequent reloading in rats. *BMC Musculoskelet. Disord.* **19**, 223 (2018).
 130. Aarden, E. M., Nijweide, P. J. & Burger, E. H. Function of osteocytes in bone. *J. Cell. Biochem.* **55**, 287–299 (1994).
 131. Moriishi, T. *et al.* Overexpression of Bcl2 in osteoblasts inhibits osteoblast differentiation and induces osteocyte apoptosis. *PLoS One* **6**, e27487–e27487

- (2011).
132. Jepsen, K. J., Silva, M. J., Vashishth, D., Guo, X. E. & van der Meulen, M. C. H. Establishing biomechanical mechanisms in mouse models: practical guidelines for systematically evaluating phenotypic changes in the diaphyses of long bones. *J. Bone Miner. Res.* **30**, 951–966 (2015).
 133. Weatherholt, A. M., Fuchs, R. K. & Warden, S. J. Cortical and trabecular bone adaptation to incremental load magnitudes using the mouse tibial axial compression loading model. *Bone* **52**, 372–379 (2013).
 134. Schaffler, M. B. & Kennedy, O. D. Osteocyte Signaling in Bone. *Curr. Osteoporos. Rep.* **10**, 118–125 (2012).
 135. Verborgt, O., Gibson, G. J. & Schaffler, M. B. Loss of Osteocyte Integrity in Association with Microdamage and Bone Remodeling After Fatigue In Vivo. *J. Bone Miner. Res.* **15**, 60–67 (2000).
 136. Wang, H. *et al.* Osteocyte-viability-based simulations of trabecular bone loss and recovery in disuse and reloading. *Biomech. Model. Mechanobiol.* **13**, 153–166 (2014).
 137. Pantschenko, A. G. *et al.* Effect of Osteoblast-Targeted Expression of Bcl-2 in Bone: Differential Response in Male and Female Mice. *J. Bone Miner. Res.* **20**, 1414–1429 (2005).
 138. Tatsumi, S. *et al.* Targeted Ablation of Osteocytes Induces Osteoporosis with Defective Mechanotransduction. *Cell Metab.* **5**, 464–475 (2007).
 139. Terpstra, A. H. M. Differences between Humans and Mice in Efficacy of the Body Fat Lowering Effect of Conjugated Linoleic Acid: Role of Metabolic Rate. *J. Nutr.* **131**, 2067–2068 (2001).
 140. Agoston, D. V. How to Translate Time? The Temporal Aspect of Human and Rodent Biology. *Front. Neurol.* **8**, 92 (2017).